International Journal of Bifurcation and Chaos, Vol. 23, No. 11 (2013) 1350180 (26 pages)

DOI: 10.1142/S0218127413501800

COMPLEX DYNAMICAL ANALYSIS OF A COUPLED NETWORK FROM INNATE IMMUNE RESPONSES

JINYING TAN* and XIUFEN ZOU†
School of Mathematics and Statistics,
Wuhan University, Wuhan 430072, P. R. China
**College of Science, Huazhong Agricultural University,*
Wuhan 430070, P. R. China
†*xfzou@whu.edu.cn*

Received February 3, 2013; Revised May 6, 2013

In this paper, we investigate the complex dynamical behaviors of a biological network that is derived from innate immune responses and that couples positive and negative feedback loops. The stability conditions of the non-negative equilibrium points (EPs) of the system are obtained, using the theory of dynamical systems, and we deduce that no more than three stable EPs exist in this system. Through bifurcation analysis and numerical simulations, we find that the system presents rich dynamical behaviors, such as monostability, bistability and oscillations. These results reveal how positive and negative feedback cooperatively regulate the dynamical behavior of the system.

Keywords: Dynamical behavior; positive and negative feedback loops; dynamical theory; bifurcation analysis.

1. Introduction

Feedback is a universal mechanism for the appropriate regulation of various cellular processes. Moreover, feedback has the potential to induce complex dynamical behaviors such as multistability, hysteresis or oscillation, which have been investigated in theory and experiments in recent years [Milo *et al.*, 2002; Ferrell, 2002; Shen-Orr *et al.*, 2002; McMillen *et al.*, 2002; Pomerening *et al.*, 2005; Iranfar *et al.*, 2006; Song *et al.*, 2007; Pfeuty & Kaneko, 2009]. Therefore, it is very important to understand the function of feedback for synthetic biology, the goal of which is to design and synthesize biological networks that perform expected behaviors in a controllable manner [Elowitz & Leibler, 2000; Endy, 2005; Alon, 2006; Andrianantoandro *et al.*, 2006; Serrano, 2007; Haseloff & Ajioka, 2009].

It is convenient to analyze the properties of biological networks according to their feedback structure. While a single feedback loop has been well studied, for example, positive feedback is the necessary condition to produce bistability [Thomas, 1994; Snoussi, 1998; Gardner *et al.*, 2000] and negative feedback can induce oscillations [Novák & Tyson, 2008], a generalization of these results for more complex networks is usually not explicit. More complex systems, coupled with positive and negative feedback loops, have been of interest to the scientific community [Cinquin & Demongeot, 2002; Süel *et al.*, 2006; Guantes & Poyatos, 2006; Song *et al.*, 2007; Novák & Tyson, 2008; Zhang *et al.*, 2010]. For example, a positive feedback network coupled with a negative feedback loop can produce a robust and adjustable oscillation

†Author for correspondence

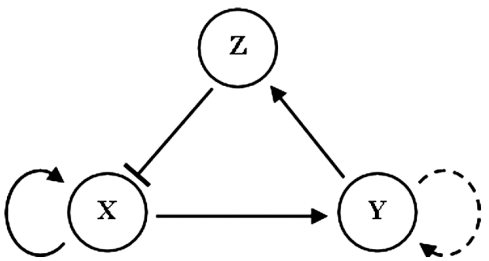

Fig. 1. A schematic diagram of a specific regulatory network with negative feedback coupled with one auto-feedback and one positive feedback. A line with an arrow indicates positive regulation, and a line with a short bar represents negative regulation. A dashed line means that there are multistep reactions.

[Stricker *et al.*, 2008; Tian *et al.*, 2009] or can obtain widely adjustable frequency and near-constant amplitude [Tsai *et al.*, 2008].

However, the generation mechanisms for how specific dynamics can be induced by feedback in biological networks with interlinked positive and negative feedback loops are still not very clear except in a few studies [Qiu & Zhou, 2012]. Therefore, this paper intends to investigate the complex dynamical behaviors of a specific regulatory network that comprises one negative feedback coupled with one auto-feedback and one positive feedback (Fig. 1), which is derived from the virus-triggered innate immune regulatory network studied in a recent study [Tan *et al.*, 2012] based on mathematical modeling validated by biological experiments. To reveal the mechanisms of generating complex dynamics, we use dynamical theory and bifurcation analysis to simulate various possible dynamical phenomena that are induced by the coupled network. These results provide new insights into mechanisms of interlinked networks and designing artificial function modules in biological systems.

2. Mathematical Model

In the schematic diagram of the regulatory network (Fig. 1), X activates Y, Y activates Z and Z inhibits X; therefore, a negative feedback loop is formed. X has an auto-feedback (or self-replication), and there exists a positive feedback by multistep reactions from Y to Y. Based on the law of mass action, we assume that the production rates (k_1, k_2 and k_3) and the degradation rates (d_1, d_2 and d_3) of the three components are linearly proportional to their concentrations. The processes of Z inhibiting X and the positive feedback of Y are represented using Hill functions. In this paradigm, the dynamics of this network is determined by a system of nonlinear ordinary differential equations (ODEs) [Tan *et al.*, 2012]:

$$\begin{cases} \dfrac{dX(t)}{dt} = k_1 X(t) \cdot \dfrac{b_1 K_1^{n_1}}{K_1^{n_1} + Z^{n_1}(t)} - d_1 X(t) \\ \dfrac{dY(t)}{dt} = k_2 X(t) + \dfrac{b_2 Y^{n_2}(t-\tau)}{K_2^{n_2} + Y^{n_2}(t-\tau)} - d_2 Y(t) \\ \dfrac{dZ(t)}{dt} = k_3 Y(t) - d_3 Z(t), \end{cases} \tag{1}$$

where $X(t)$, $Y(t)$ and $Z(t)$ are the concentrations of three components, X, Y and Z, respectively. K_1 and K_2 are the inhibition and activation coefficients of Z and Y, respectively; b_1 and b_2 are the maximal production rates and n_1 and n_2 are the Hill coefficients in two Hill functions, respectively. The multistep reaction processes in the positive feedback of Y are omitted and are substituted by a time delay τ.

For brevity and clarity, we let $\tau = 0$ and nondimensionalize system (1). Time is scaled relative to the degradation rate (d_3) of Z. We make the following substitutions and assume that all of the model parameters are greater than 0 for studying the actual biological significance.

$$x(t) = \frac{k_2 k_3}{K_1 d_3^2} X(t), \quad y(t) = \frac{k_3}{K_1 d_3} Y(t),$$

$$z(t) = \frac{1}{K_1} Z(t), \quad \bar{t} = d_3 t, \quad K = \frac{k_3}{K_1 d_3} K_2,$$

$$\alpha_1 = \frac{k_1 b_1}{d_3}, \quad \alpha_2 = \frac{d_1}{d_3}, \quad \alpha_3 = \frac{k_3 b_2}{K_1 d_3^2},$$

$$\alpha_4 = \frac{d_2}{d_3}, \quad \sigma_1 = \frac{\alpha_1}{\alpha_2} = \frac{k_1 b_1}{d_1}, \quad \sigma_2 = \frac{\alpha_3}{\alpha_4}.$$

Using t instead of $\bar{t}$ for notational convenience, we obtain the nondimensional system of equations:

$$\begin{cases} \dfrac{dx(t)}{dt} = \dfrac{\sigma_1 \alpha_2 x(t)}{1 + z^{n_1}(t)} - \alpha_2 x(t) \\ \dfrac{dy(t)}{dt} = x(t) + \dfrac{\sigma_2 \alpha_4 y^{n_2}(t)}{K^{n_2} + y^{n_2}(t)} - \alpha_4 y(t) \\ \dfrac{dz(t)}{dt} = y(t) - z(t), \end{cases} \tag{2}$$

where $x(t)$, $y(t)$ and $z(t)$ are the dimensionless concentrations of the components X, Y and Z, respectively. System (2) is determined by five dimensionless parameters σ_1, σ_2, α_2, α_4 and K and the two Hill coefficients, n_1 and n_2. The variables α_2 and α_4 are called the relative degradation ratios. K is the relative activation coefficient of Y. Additionally, σ_1 can be viewed as the relative ratio between the auto-feedback and the negative feedback strengths, i.e. the auto-negative ratio, and σ_2 can be viewed as the relative strength of the positive feedback loop.

Considering the biological significance, we assume that all of the parameters are greater than 0 and that n_1 and n_2 take on positive integer values. From system (2), we can see that σ_1 and σ_2 are two important parameters that are related to the positive and negative feedback. Therefore, most of the analysis and simulations in the following sections are based on the two parameters.

3. Theoretical Analysis

We primarily use the basic stability principle in a dynamical system [Hale, 1977] and Routh–Hurwitz criterion [Dorf & Bishop, 2001] to analyze the stability conditions of the equilibrium points (EPs) of system (2). At the same time, using the methods in [Kuznetsov, 1998; Liu & Liu, 2012], we discuss some typical bifurcations for system (2).

3.1. *Case 1*: *Hill coefficient* $n_2 = 1$

When $n_2 = 1$, system (2) can be simplified as follows

$$\begin{cases} \dfrac{dx(t)}{dt} = \dfrac{\sigma_1\alpha_2 x(t)}{1+z^{n_1}(t)} - \alpha_2 x(t) \\ \dfrac{dy(t)}{dt} = x(t) + \dfrac{\sigma_2\alpha_4 y(t)}{K+y(t)} - \alpha_4 y(t) \\ \dfrac{dz(t)}{dt} = y(t) - z(t). \end{cases} \tag{3}$$

Then we easily obtain the three non-negative EPs of system (3) (the second column in Table 1) and infer the following results about the stability conditions for the system in (3):

Theorem 1. *There exist three non-negative EPs for system (3), and only one EP is locally asymptotically stable under any one of the following conditions (detailed proofs are presented in Appendix A):*

(1) *If* $\sigma_1 < 1$ *and* $\sigma_2 < K$, *then system (3) is locally asymptotically stable at the first EP* $E_1^{n_1,1}$.

(2) *If* $\sigma_2 > \max\{K, K + (\sigma_1 - 1)^{\frac{1}{n_1}}\}$, *then system (3) is locally asymptotically stable at the second EP* $E_2^{n_1,1}$.

(3) *If* $\sigma_1 > 1$, $\sigma_2 < K + (\sigma_1 - 1)^{\frac{1}{n_1}}$ *and* $\alpha_2 < C^{n_1,1}$, *then system (3) is locally asymptotically stable at the third EP* $E_3^{n_1,1}$, *where*

$$C^{n_1,1} = \frac{\sigma_1}{n_1(\sigma_1-1)} \cdot \left\{ 1 + \alpha_4 - \frac{K\sigma_2\alpha_4}{\left[K + (\sigma_1-1)^{\frac{1}{n_1}}\right]^2} \right\} \cdot \frac{K + (\sigma_1-1)^{\frac{1}{n_1}} - \dfrac{K\sigma_2}{K + (\sigma_1-1)^{\frac{1}{n_1}}}}{K + (\sigma_1-1)^{\frac{1}{n_1}} - \sigma_2}.$$

We summarize the stability conditions for system (3) at the EPs in Table 1 ($\sigma_1, \sigma_2, \alpha_2, \alpha_4$, and K are greater than 0) when $n_2 = 1$.

To easily observe the stable regions, a theoretical diagram of stability about parameters σ_1 and σ_2 is depicted in Fig. 2 when $n_2 = 1$. The first quadrant in the plane σ_1–σ_2 is divided into three regions, A, B and C, by the lines $\sigma_1 = 1$ and $\sigma_2 = K$ and the curve $\sigma_2 = K + (\sigma_1 - 1)^{\frac{1}{n_1}}$, and the quasi-parabolic curve in Fig. 2(a) degenerates into a straight line in Fig. 2(b) when $n_1 = 1$; however, the basic form in Fig. 2(b) corresponds to Fig. 2(a). In each stable region, there is only one stable EP, and the perturbation of parameters n_1, K, α_2 and α_4 will not change the basic structure of the diagram, which indicates that system (3) is robust about these parameters. However, because of different positive and negative feedback strengths, there are different biological behaviors in different regions. When the relative ratio σ_1 and the relative strength of the positive feedback σ_2 are small ($\sigma_1 < 1$ and $\sigma_2 < K$), then three components will tend to zero when the initial point is near the origin, which corresponds to region A (Table 1). When σ_1 and σ_2 satisfy other conditions, system (3) can reach the other two equilibrium states (region B or region C in Fig. 2 and Table 1).

From the proof of Theorem 1, we can observe that the EPs $E_1^{n_1,1}$ and $E_3^{n_1,1}$ collide, forming an

Table 1. The stability conditions at the non-negative EPs ($n_2 = 1$).

EPs	$(\overline{x}, \overline{y}, \overline{z})$	Stability Conditions	Domain in Fig. 2	Additional Conditions
$E_1^{n_1,1}$	$(0,0,0)$	$\sigma_1 < 1, \quad \sigma_2 < K$	A	—
$E_2^{n_1,1}$	$(0, \sigma_2 - K, \sigma_2 - K)$	$\sigma_2 > K, \quad \sigma_2 > K + (\sigma_1 - 1)^{\frac{1}{n_1}} \quad (\sigma_1 \geq 1)$	B	—
$E_3^{n_1,1}$	$\left(\alpha_4(\sigma_1 - 1)^{\frac{1}{n_1}}\left[1 - \frac{\sigma_2}{K + (\sigma_1 - 1)^{\frac{1}{n_1}}}\right], (\sigma_1 - 1)^{\frac{1}{n_1}}, (\sigma_1 - 1)^{\frac{1}{n_1}}\right)$	$\sigma_1 > 1, \quad \sigma_2 < K + (\sigma_1 - 1)^{\frac{1}{n_1}}$	C	$\alpha_2 < C^{n_1,1}$

equilibrium (the origin) at $\sigma_1 = 1$ when $\sigma_2 < K$. The exchange of the stability of $E_1^{n_1,1}$ and $E_3^{n_1,1}$ occurs as σ_1 passes through 1, i.e. $E_1^{n_1,1}$ is stable and $E_3^{n_1,1}$ is unstable when $\sigma_1 < 1$; however, $E_1^{n_1,1}$ is unstable and $E_3^{n_1,1}$ is stable when $\sigma_1 > 1$, which indicates that a codimension-one transcritical bifurcation (TB) at the origin takes place. Performing the same analysis, we have a similar codimension-one bifurcation about parameter σ_1 at $E_2^{n_1,1}$ in the case $\sigma_1 = 1 + (\sigma_2 - K)^{n_1}$ and $\sigma_2 > K$ or parameter σ_2 [Theorems 2(1) and 2(2)]. When $\sigma_1 = 1$ and $\sigma_2 = K$, the three equilibria $E_1^{n_1,1}$, $E_2^{n_1,1}$ and $E_3^{n_1,1}$ collide at the origin and the linearized system of (3) has two eigenvalues $\lambda_1 = \lambda_2 = 0$ and a negative eigenvalue $\lambda_3 = -1$ at the origin, which means that the origin is a codimension-two bifurcation (Bogdanov–Takens bifurcation (BTB)) point in the case where $\sigma_1 = 1$ and $\sigma_2 = K$ [Theorem 2(3)]. To investigate the bifurcation of the limit cycles in system (3) about the parameters σ_1 or σ_2, we introduce the following lemma:

Lemma 1. *If α_2 is viewed as a bifurcation parameter, then a Hopf bifurcation occurs as α_2 passes through C^{n_1,n_2} for the system in (2) (detailed proofs are presented in Appendix B).*

Let $\alpha_2 = \alpha_2(\sigma_1, \sigma_2) = C^{n_1,n_2}$. Because $\alpha_2(\sigma_1, \sigma_2) \neq const.$, there exists a σ_1^{HB} or σ_2^{HB} that satisfies $\frac{d\alpha_2}{d\sigma_1}|_{\sigma_1=\sigma_1^{HB}} \neq 0$ or $\frac{d\alpha_2}{d\sigma_2}|_{\sigma_2=\sigma_2^{HB}} \neq 0$, respectively, then the transversality condition

$$\begin{aligned}
&\mathrm{Re}\left(\frac{d\lambda_1}{d\sigma_1}\right)\Big|_{\sigma_1=\sigma_1^{HB}} \\
&\quad = \mathrm{Re}\left(\frac{d\lambda_1}{d\alpha_2}\Big|_{\alpha_2=C^{n_1,n_2}} \cdot \frac{d\alpha_2}{d\sigma_1}\Big|_{\sigma_1=\sigma_1^{HB}}\right) \\
&\quad = \frac{d\alpha_2}{d\sigma_1}\Big|_{\sigma_1=\sigma_1^{HB}} \cdot \mathrm{Re}\left(\frac{d\lambda_1}{d\alpha_2}\Big|_{\alpha_2=C^{n_1,n_2}}\right) \neq 0
\end{aligned}$$

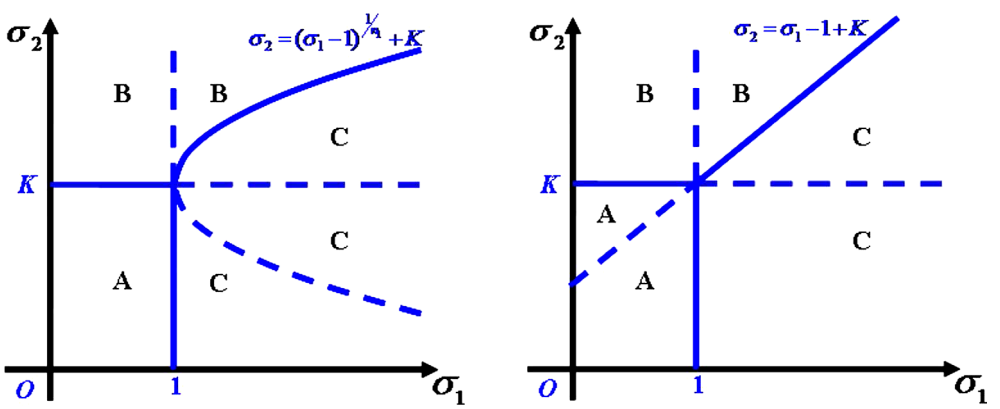

(a) (b)

Fig. 2. Stable regions when $n_2 = 1$. The first quadrant in the plane σ_1–σ_2 is divided into three regions, A, B and C, by the lines $\sigma_1 = 1$ and $\sigma_2 = K$ and the curve $\sigma_2 = K + (\sigma_1 - 1)^{\frac{1}{n_1}}$. (a) $n_1 > 1$ and (b) $n_1 = 1$. The quasi-parabolic curve in (a) degenerates into a straight line, but the basic form in (b) corresponds to (a).

or

$$\begin{aligned}&\mathrm{Re}\left(\frac{d\lambda_1}{d\sigma_2}\right)\Big|_{\sigma_2=\sigma_2^{HB}}\\&\quad=\mathrm{Re}\left(\frac{d\lambda_1}{d\alpha_2}\Big|_{\alpha_2=C^{n_1,n_2}}\cdot\frac{d\alpha_2}{d\sigma_2}\Big|_{\sigma_2=\sigma_2^{HB}}\right)\\&\quad=\frac{d\alpha_2}{d\sigma_2}\Big|_{\sigma_2=\sigma_2^{HB}}\cdot\mathrm{Re}\left(\frac{d\lambda_1}{d\alpha_2}\Big|_{\alpha_2=C^{n_1,n_2}}\right)\neq 0\end{aligned}$$

is satisfied; in other words, a Hopf bifurcation occurs as σ_1 or σ_2 passes through σ_1^{HB} or σ_2^{HB} for system (3) [and for system (2)] if σ_1 or σ_2 is viewed as a bifurcation parameter [Theorem 2(4)].

Thus, we have the following bifurcation results (Theorem 2 and Table 2) when $n_2 = 1$:

Theorem 2. *Assume that σ_1 or σ_2 are bifurcation parameters when the other parameters are fixed, and we have*

(1) *The system in (3) goes through a transcritical bifurcation (TB) at the origin in the case where $\sigma_1 = 1$ and $\sigma_2 < K$, or at EP $(0, (\sigma_1 - 1)^{\frac{1}{n_1}}, (\sigma_1 - 1)^{\frac{1}{n_1}})$ in the case where $\sigma_1 = 1 + (\sigma_2 - K)^{n_1}$ and $\sigma_2 > K$.*
(2) *The system in (3) goes through a transcritical bifurcation (TB) at the origin in the case where $\sigma_2 = K$ and $\sigma_1 < 1$, or at EP $(0, (\sigma_1 - 1)^{\frac{1}{n_1}}, (\sigma_1 - 1)^{\frac{1}{n_1}})$ in the case where $\sigma_2 = K + (\sigma_1 - 1)^{\frac{1}{n_1}}$ and $\sigma_1 > 1$.*
(3) *The system in (3) goes through a codimension-two Bogdanov–Takens bifurcation (BTB) at the origin in the case where $\sigma_1 = 1$ and $\sigma_2 = K$.*
(4) *The system in (3) goes through a Hopf bifurcation (HB) at $E_3^{n_1,1}$ as σ_1 passes through some σ_1^{HB} or as σ_2 passes through some σ_2^{HB}, where σ_1^{HB} or σ_2^{HB} satisfies $\alpha_2(\sigma_1^{HB}, \sigma_2) = C^{n_1,1}$ or $\alpha_2(\sigma_1, \sigma_2^{HB}) = C^{n_1,1}$, respectively.*

The above bifurcation analysis shows that the variety of auto-feedback or positive feedback strength will cause dramatic changes in the behaviors of the system.

3.2. *Case 2*: *Hill coefficient* $n_2 > 1$

If the Hill coefficient $n_2 > 1$ in system (2), then we easily obtain four non-negative EPs of system (2) (the second column in Table 3).

We have the following results on the stability conditions for system (2) when $n_2 > 1$:

Theorem 3. *System (2) has three non-negative stable EPs under certain conditions and an unstable EP (detailed proofs are presented in Appendix C):*

(1) *If $\sigma_1 < 1$, then system (2) is locally asymptotically stable at the first EP $E_1^{n_1,n_2}$.*
(2) *The second EP $E_{21}^{n_1,n_2}$ is always unstable.*
(3) *If*

$$\sigma_2 > \frac{n_2 K}{(n_2-1)^{\frac{n_2-1}{n_2}}} \quad \text{and}$$

$$\sigma_2 > \frac{K^{n_2} + (\sigma_1 - 1)^{\frac{n_2}{n_1}}}{(\sigma_1 - 1)^{\frac{n_2-1}{n_1}}}$$

$$(\sigma_1 \geq 1 + (n_2 - 1)^{\frac{n_2}{n_2}} K^{n_1}),$$

then system (2) is locally asymptotically stable at the third EP $E_{22}^{n_1,n_2}$.

Table 2. Bifurcation values and types ($n_2 = 1$).

Parameters	Conditions	Values	Type	
σ_1	$\sigma_2 < K$	1	TB	
	$\sigma_2 > K$	$1 + (\sigma_2 - K)^{n_1}$	TB	
	$\alpha_2(\sigma_1^{HB}, \sigma_2) = C^{n_1,1}$	σ_1^{HB}	HB	
σ_2	$\sigma_1 < 1$	K	TB	Codimen one
	$\sigma_1 > 1$	$K + (\sigma_1 - 1)^{\frac{1}{n_1}}$	TB	
	$\alpha_2(\sigma_1, \sigma_2^{HB}) = C^{n_1,1}$	σ_2^{HB}	HB	
σ_1 & σ_2		$\sigma_1 = 1$ & $\sigma_2 = K$	BTB	Codimen two

Table 3. The stability conditions at the non-negative EPs ($n_2 > 1$).

EPs	$(\overline{x}, \overline{y}, \overline{z})$	Stability Conditions	Domain in Fig. 3	Additional Conditions
$E_1^{n_1,n_2}$	$(0,0,0)$	$\sigma_1 < 1$	A B	—
$E_{21}^{n_1,n_2}$	$(0, \overline{y}_{21}^{n_1,n_2}, \overline{z}_{21}^{n_1,n_2} (= \overline{y}_{21}^{n_1,n_2}))$	—	—	—
$E_{22}^{n_1,n_2}$	$(0, \overline{y}_{22}^{n_1,n_2}, \overline{z}_{22}^{n_1,n_2} (= \overline{y}_{22}^{n_1,n_2}))$	$\sigma_2 > \dfrac{n_2 K}{(n_2-1)^{\frac{n_2-1}{n_2}}}$, $\sigma_2 > \dfrac{K^{n_2} + (\sigma_1-1)^{\frac{n_2}{n_1}}}{(\sigma_1-1)^{\frac{n_2-1}{n_1}}}$ $(\sigma_1 \geq 1 + (n_2-1)^{\frac{n_1}{n_2}} K^{n_1})$	B C D	—
$E_3^{n_1,n_2}$	$\left(\alpha_4 \left[(\sigma_1-1)^{\frac{1}{n_1}} - \dfrac{\sigma_2(\sigma_1-1)^{\frac{n_2}{n_1}}}{K^{n_2} + (\sigma_1-1)^{\frac{n_2}{n_1}}}\right], (\sigma_1-1)^{\frac{1}{n_1}}, (\sigma_1-1)^{\frac{1}{n_1}}\right)$	$\sigma_1 > 1$, $\sigma_2 < \min\left\{ \dfrac{K^{n_2} + (\sigma_1-1)^{\frac{n_2}{n_1}}}{(\sigma_1-1)^{\frac{n_2-1}{n_1}}}, \dfrac{\left[K^{n_2} + (\sigma_1-1)^{\frac{n_2}{n_1}}\right]^2}{n_2 K^{n_2} (\sigma_1-1)^{\frac{n_2-1}{n_1}}} \right\}$	C F	$\alpha_2 < C^{n_1,n_2}$

(4) If

$$\sigma_1 > 1, \quad \sigma_2 < \min\left\{ \frac{K^{n_2} + (\sigma_1-1)^{\frac{n_2}{n_1}}}{(\sigma_1-1)^{\frac{n_2-1}{n_1}}}, \frac{\left[K^{n_2} + (\sigma_1-1)^{\frac{n_2}{n_1}}\right]^2}{n_2 K^{n_2} (\sigma_1-1)^{\frac{n_2-1}{n_1}}} \right\}$$

and $\alpha_2 < C^{n_1,n_2}$, *then system (2) is locally asymptotically stable at the fourth EP* $E_3^{n_1,n_2}$, *where*

$$C^{n_1,n_2} = \frac{\left\{1 + \alpha_4 - \dfrac{n_2 \sigma_2 \alpha_4 K^{n_2} (\sigma_1-1)^{\frac{n_2-1}{n_1}}}{\left[K^{n_2} + (\sigma_1-1)^{\frac{n_2}{n_1}}\right]^2}\right\} \cdot \left\{1 - \dfrac{n_2 \sigma_2 K^{n_2} (\sigma_1-1)^{\frac{n_2-1}{n_1}}}{\left[K^{n_2} + (\sigma_1-1)^{\frac{n_2}{n_1}}\right]^2}\right\}}{\dfrac{n_1(\sigma_1-1)\left[K^{n_2} + (\sigma_1-1)^{\frac{n_2}{n_1}} - \sigma_2(\sigma_1-1)^{\frac{n_2-1}{n_1}}\right]}{\sigma_1\left[K^{n_2} + (\sigma_1-1)^{\frac{n_2}{n_1}}\right]}}.$$

Similar to the above discussions, we can summarize the stability conditions for system (2) at EPs, as given in Table 3 ($\sigma_1, \sigma_2, \alpha_2, \alpha_4$, and K are greater than 0) when $n_2 > 1$.

From the stability diagram (Fig. 3) and Table 3 we can observe that when $n_2 > 1$, system (2) exhibits bistability phenomena in region B ($E_1^{n_1,n_2}$ and $E_{22}^{n_1,n_2}$) and C ($E_{22}^{n_1,n_2}$ and $E_3^{n_1,n_2}$), which does not exist in the case of $n_2 = 1$.

Similar to the case of $n_2 = 1$, from the proof of Theorem 3 we can observe that the EPs $E_1^{n_1,n_2}$ and $E_3^{n_1,n_2}$ collide, forming an equilibrium (the origin) at $\sigma_1 = 1$. The exchange of the stability of $E_1^{n_1,n_2}$ and $E_3^{n_1,n_2}$ occurs as σ_1 passes through 1, i.e. $E_1^{n_1,n_2}$ is stable and $E_3^{n_1,n_2}$ is unstable when $\sigma_1 < 1$; however, $E_1^{n_1,n_2}$ is unstable and $E_3^{n_1,n_2}$ is stable when $\sigma_1 > 1$, which indicates that system (2) goes through a codimension-one transcritical bifurcation (TB) at the origin in the case of $\sigma_1 = 1$. When $\sigma_1 > 1 + (n_2-1)^{\frac{n_1}{n_2}} K^{n_1}$ and $\sigma_2 > \frac{n_2 K}{(n_2-1)^{\frac{n_2-1}{n_2}}}$, the EPs $E_{22}^{n_1,n_2}$ and $E_3^{n_1,n_2}$ will collide, forming an

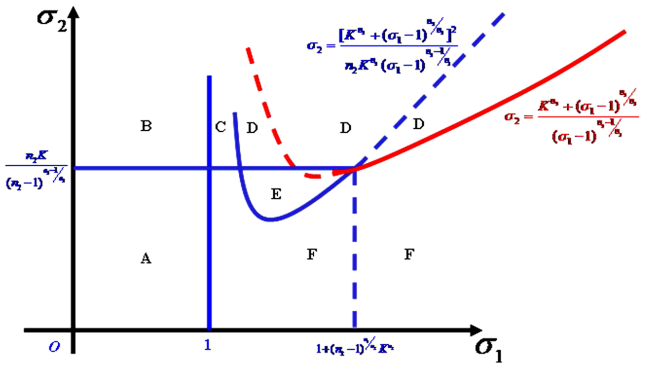

Fig. 3. Stable regions when $n_2 > 1$. The first quadrant in the plane σ_1–σ_1 is divided into six regions, A–F, by the lines $\sigma_1 = 1$ and $\sigma_2 = \frac{n_2 K}{(n_2-1)^{\frac{n_2-1}{n_2}}}$, and the curves $\sigma_2 = \frac{K^{n_2}+(\sigma_1-1)^{\frac{n_2}{n_1}}}{(\sigma_1-1)^{\frac{n_2-1}{n_1}}}$ and $\sigma_2 = \frac{[K^{n_2}+(\sigma_1-1)^{\frac{n_2}{n_1}}]^2}{n_2 K^{n_2}(\sigma_1-1)^{\frac{n_2-1}{n_1}}}$.

equilibrium $(0,(\sigma_1-1)^{\frac{1}{n_1}},(\sigma_1-1)^{\frac{1}{n_1}})$ at σ_1^{TB}, where σ_1^{TB} satisfies $\sigma_2 = \frac{K^{n_2}+(\sigma_1^{TB}-1)^{\frac{n_2}{n_1}}}{(\sigma_1^{TB}-1)^{\frac{n_2-1}{n_1}}}$. The exchange of the stability of $E_{22}^{n_1,n_2}$ and $E_3^{n_1,n_2}$ occurs as σ_1 passes through σ_1^{TB}, i.e. $E_{22}^{n_1,n_2}$ is stable and $E_3^{n_1,n_2}$ is unstable when $\sigma_1 < \sigma_1^{TB}$; however, $E_{22}^{n_1,n_2}$ is unstable and $E_3^{n_1,n_2}$ is stable when $\sigma_1 > \sigma_1^{TB}$, which indicates that system (2) also undergoes a codimension-one transcritical bifurcation (TB) at EP $(0,(\sigma_1-1)^{\frac{1}{n_1}},(\sigma_1-1)^{\frac{1}{n_1}})$ in case $\sigma_1 = \sigma_1^{TB}$ when $\sigma_2 > \frac{n_2 K}{(n_2-1)^{\frac{n_2-1}{n_2}}}$ [Theorem 4(1)].

For parameter σ_2, the stable equilibrium point $E_{22}^{n_1,n_2}$ and unstable equilibrium point $E_{21}^{n_1,n_2}$ when $\sigma_2 > \frac{n_2 K}{(n_2-1)^{\frac{n_2-1}{n_2}}}$ and $\sigma_1 < 1+(n_2-1)^{\frac{n_1}{n_2}}K^{n_1}$ will collide together at $\sigma_2 = \frac{n_2 K}{(n_2-1)^{\frac{n_2-1}{n_2}}}$, forming another codimension one saddle-node bifurcation (SNB). When $\sigma_1 > 1+(n_2-1)^{\frac{n_1}{n_2}}K^{n_1}$, EPs $E_{22}^{n_1,n_2}$ and $E_3^{n_1,n_2}$ will collide, forming an equilibrium $(0,(\sigma_1-1)^{\frac{1}{n_1}},(\sigma_1-1)^{\frac{1}{n_1}})$ at $\sigma_2^{TB} = \frac{K^{n_2}+(\sigma_1-1)^{\frac{n_2}{n_1}}}{(\sigma_1-1)^{\frac{n_2-1}{n_1}}}$. The exchange of the stability of $E_{22}^{n_1,n_2}$ and $E_3^{n_1,n_2}$ occurs as σ_2 passes through σ_2^{TB}, i.e. $E_{22}^{n_1,n_2}$ is stable and $E_3^{n_1,n_2}$ is unstable when $\sigma_2 > \sigma_2^{TB}$; however, $E_{22}^{n_1,n_2}$ is unstable and $E_3^{n_1,n_2}$ is stable when $\sigma_2 < \sigma_2^{TB}$, which indicates that system (2) also undergoes a codimension-one transcritical bifurcation (TB) at EP $(0,(\sigma_1-1)^{\frac{1}{n_1}},(\sigma_1-1)^{\frac{1}{n_1}})$ in the case where $\sigma_2 = \frac{K^{n_2}+(\sigma_1-1)^{\frac{n_2}{n_1}}}{(\sigma_1-1)^{\frac{n_2-1}{n_1}}}$ when $\sigma_1 > 1+(n_2-1)^{\frac{n_1}{n_2}}K^{n_1}$ [Theorem 4(2)].

The bifurcation of the limit cycles in system (2) about parameter σ_1 or σ_2 is similar to Theorem 2(4), and we have Theorem 4(3). Thus, we have the following bifurcation results (Theorem 4 and Table 4) when $n_2 > 1$:

Theorem 4. *Assume that σ_1 or σ_2 are bifurcation parameters when the other parameters are fixed, and we have*

(1) *The system in (2) goes through a transcritical bifurcation (TB) at the origin in the case where $\sigma_1 = 1$, or at EP $(0,(\sigma_1-1)^{\frac{1}{n_1}},(\sigma_1-1)^{\frac{1}{n_1}})$ as σ_1*

Table 4. Bifurcation values and types ($n_2 > 1$).

Parameters	Conditions	Values	Type	
σ_1		1	TB	Codimen one
	$\sigma_2 = \frac{K^{n_2}+(\sigma_1^{TB}-1)^{\frac{n_2}{n_1}}}{(\sigma_1^{TB}-1)^{\frac{n_2-1}{n_1}}}$	σ_1^{TB}	TB	
	$\alpha_2(\sigma_1^{HB},\sigma_2) = C^{n_1,n_2}$	σ_1^{HB}	HB	
σ_2	$\sigma_1 < 1+(n_2-1)^{\frac{n_1}{n_2}}K^{n_1}$	$\frac{n_2 K}{(n_2-1)^{\frac{n_2-1}{n_2}}}$	SNB	
	$\sigma_1 > 1+(n_2-1)^{\frac{n_1}{n_2}}K^{n_1}$	$\frac{K^{n_2}+(\sigma_1-1)^{\frac{n_2}{n_1}}}{(\sigma_1-1)^{\frac{n_2-1}{n_1}}}$	TB	
	$\alpha_2(\sigma_1,\sigma_2^{HB}) = C^{n_1,n_2}$	σ_2^{HB}	HB	

passes through σ_1^{TB}, *where* σ_1^{TB} *satisfies* $\sigma_2 = \frac{K^{n_2}+(\sigma_1^{TB}-1)^{\frac{n_2}{n_1}}}{(\sigma_1^{TB}-1)^{\frac{n_2-1}{n_1}}}$ *and* $\sigma_1^{TB} > 1 + (n_2-1)^{\frac{n_1}{n_2}} K^{n_1}$.

(2) *The system in* (2) *goes through a transcritical bifurcation* (*TB*) *at EP* $(0, (\sigma_1-1)^{\frac{1}{n_1}}, (\sigma_1-1)^{\frac{1}{n_1}})$ *as* σ_2 *passes through* $\frac{K^{n_2}+(\sigma_1-1)^{\frac{n_2}{n_1}}}{(\sigma_1-1)^{\frac{n_2-1}{n_1}}}$ *when* $\sigma_1 > 1 + (n_2-1)^{\frac{n_1}{n_2}} K$, *or the system in* (2) *goes through saddle-node bifurcation* (*SNB*) *at* $E_{22}^{n_1,n_2}$ $(= E_{21}^{n_1,n_2})$ *as* σ_2 *passes through* $\frac{n_2 K}{(n_2-1)^{\frac{n_2-1}{n_2}}}$ *when* $\sigma_1 < 1 + (n_2-1)^{\frac{n_1}{n_2}} K^{n_1}$.

(3) *The system in* (2) *goes through a Hopf bifurcation* (*HB*) *at* $E_3^{n_1,n_2}$ *as* σ_1 *passes through some* σ_1^{HB} *or* σ_2 *passes through some* σ_2^{HB}, *where* σ_1^{HB} *or* σ_2^{HB} *satisfies with* $\alpha_2(\sigma_1^{HB}, \sigma_2) = C^{n_1,n_2}$ *or* $\alpha_2(\sigma_1, \sigma_2^{HB}) = C^{n_1,n_2}$, *respectively.*

4. Numerical Results and Discussions

4.1. *Global bifurcation analysis with two parameters*

To understand the influences of feedback on the dynamical behaviors of the system (2), we depict a two-parameter bifurcation diagram in the plane σ_1–σ_2 using AUTO software [Ermentrout, 2002] (see Fig. 4). The first quadrant is divided into a number of regions, the monostable region (M), the bistable region (B) or the oscillatory region (O). When $n_2 = 1$, the system exhibits only monostable or oscillatory behaviors, i.e. the first quadrant can simply be divided into two regions: a monostable and an oscillatory region regardless of $n_1 = 1$ or $n_1 = 2$ [see Figs. 4(a1) and 4(a2)]. When $n_2 = 2$, the system performs richer dynamical behaviors. There are not only monostable and oscillatory cases but also bistable cases [Figs. 4(b1) and 4(b2)].

The monostable region can further be divided into three subregions by the transcritical bifurcation points (TB), the stable region M1 for E_1, the stable region M2 for E_2 (or E_{22}) and the stable region M3 for E_3, regardless of $n_2 = 1$ or $n_2 = 2$. Similarly, the bistable region can be divided into two subregions by transcritical points (TB), the bistable region B1 for E_1 and E_{22} and the bistable region B2 for E_{22} and E_3 when $n_2 = 2$. These criteria indicate that the synergy among Y is the necessary condition to trigger bistability. Obviously, B2 is much narrower than B1 in Figs. 4(b1) and 4(b2), and oscillation at different values of n_2 also exhibits different forms. When $n_2 = 1$, the supercritical Hopf bifurcation points form an oscillating region (O) [see the lower right region in Figs. 4(a1) and 4(a2)]. Similarly, when $n_2 = 2$, the supercritical Hopf bifurcation points can also enclose an oscillating region in the lower right in Figs. 4(b1) and 4(b2). There are two disconnected oscillating subregions when $n_1 = 1$ [Fig. 4(b1)], but these two subregions merge into a larger oscillating region together when $n_1 = 2$ [Fig. 4(b2)]. When $n_2 = 2$, the system exhibits a supercritical Hopf bifurcation phenomenon and a subcritical Hopf bifurcation phenomenon, which show richer dynamical behaviors.

As in the discussion above, the system performs different dynamical behaviors under different cases with a synergistic effect ($n_2 = 2$) or no synergy ($n_2 = 1$) among Y. When $n_2 = 2$, i.e. there is synergy, the system behaviors are richer (monostability, bistability or oscillation), which coincides with the real-life phenomena, such as rehabilitation from the viral infection state, or the carrier or periodic state of an illness. Another example is the processes of cell life movement that present differentiation, apoptosis, replication and other phenomena. We are also concerned about the network's dynamical behaviors when n_1 and n_2 are greater than 2. From Fig. 5, we can see that various values of n_1 and n_2 do not have a large influence on the network's dynamic behaviors. Only the size of the oscillation regions is slightly larger with an increase in n_1. Therefore, in the following discussion of considering synergy in negative and positive feedback, n_1 and n_2 are set to be 2.

We also investigate the effect of the other parameters, K, α_2 or α_4, on network's dynamical behaviors. As shown in Figs. 6–8 with different Hill coefficients, we observe that the variants of these parameters do not change the structure of the global bifurcation diagram in Fig. 4 and only slightly change the boundary of the divided regions, which reflects two different trends in the plane σ_1–σ_2 in Fig. 4. An increase in K expands the oscillating region, while it reduces the monostable or bistable regions [Figs. 6(a), 7(a) and 8(a)]. The reason is that the increase in K decreases Y in the positive feedback loop and, accordingly, expands the oscillating region. An increase in α_2 has almost no impact on the network's dynamic behaviors [Figs. 6(b),

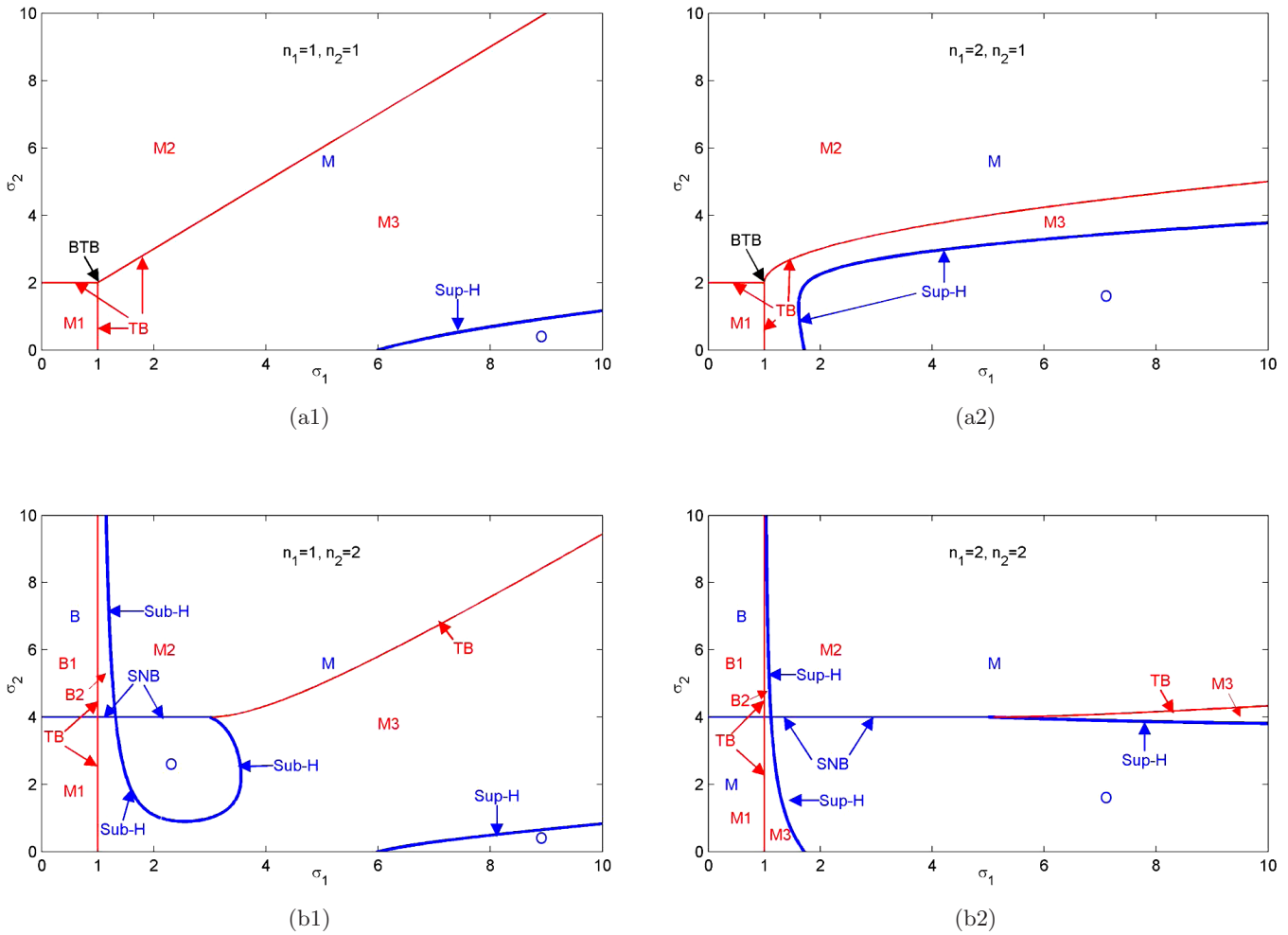

Fig. 4. Global bifurcation diagrams about σ_1 and σ_2. The abbreviations and symbols are as follows: M, a monostable region that is divided into three subregions: M1, M2 and M3; B, a bistable region that is divided into two subregions: B1 and B2; O, an oscillation region; TB, a transcritical bifurcation point; Sub-H, a subcritical Hopf bifurcation point; Sup-H, a supercritical Hopf bifurcation point; SNB, a saddle-node bifurcation point; and BTB, a Bogdanov–Takens bifurcation point. The other parameters are: $K = 2$, $\alpha_2 = 6$ and $\alpha_4 = 4$ in addition to the value of n_1 and n_2 marked in the diagram.

7(b) and 8(b)]. When α_4 is increased, the oscillation region is decreased, while the monostable or bistable regions are slightly increased [Figs. 6(c), 7(c) and 8(c)]. These results indicate that the network exhibits strong robustness for these parameter perturbations. Therefore, we mainly analyze the effect of two parameters, σ_1 and σ_2, on the network's dynamical behaviors while we fix the other three parameters to $K = 2$, $\alpha_2 = 6$ and $\alpha_4 = 4$.

4.2. *Local bifurcation analysis*

4.2.1. *Monostability and bistability*

During a certain period, the process of life always shows itself to be in a balance, i.e. a steady-state, comprising monostability and bistability (or multistability). A bistable property of a regulatory network allows an organism to better adapt to changes in the surrounding environment. Therefore, it is necessary to investigate the mechanisms for the production of monostability or bistability. Here, we investigate how the monostable and bistable states are induced by feedback.

First, from the global bifurcation graph in Fig. 4(a), without the synergy among Y ($n_2 = 1$), strong auto-feedback strength (σ_1 takes large value) easily induces oscillation. No matter how large the auto-feedback strength, however, the system can inhibit the oscillation by increasing Y's positive feedback strength (σ_2), obtaining a stable state (entering into the subegion M3). With an increase

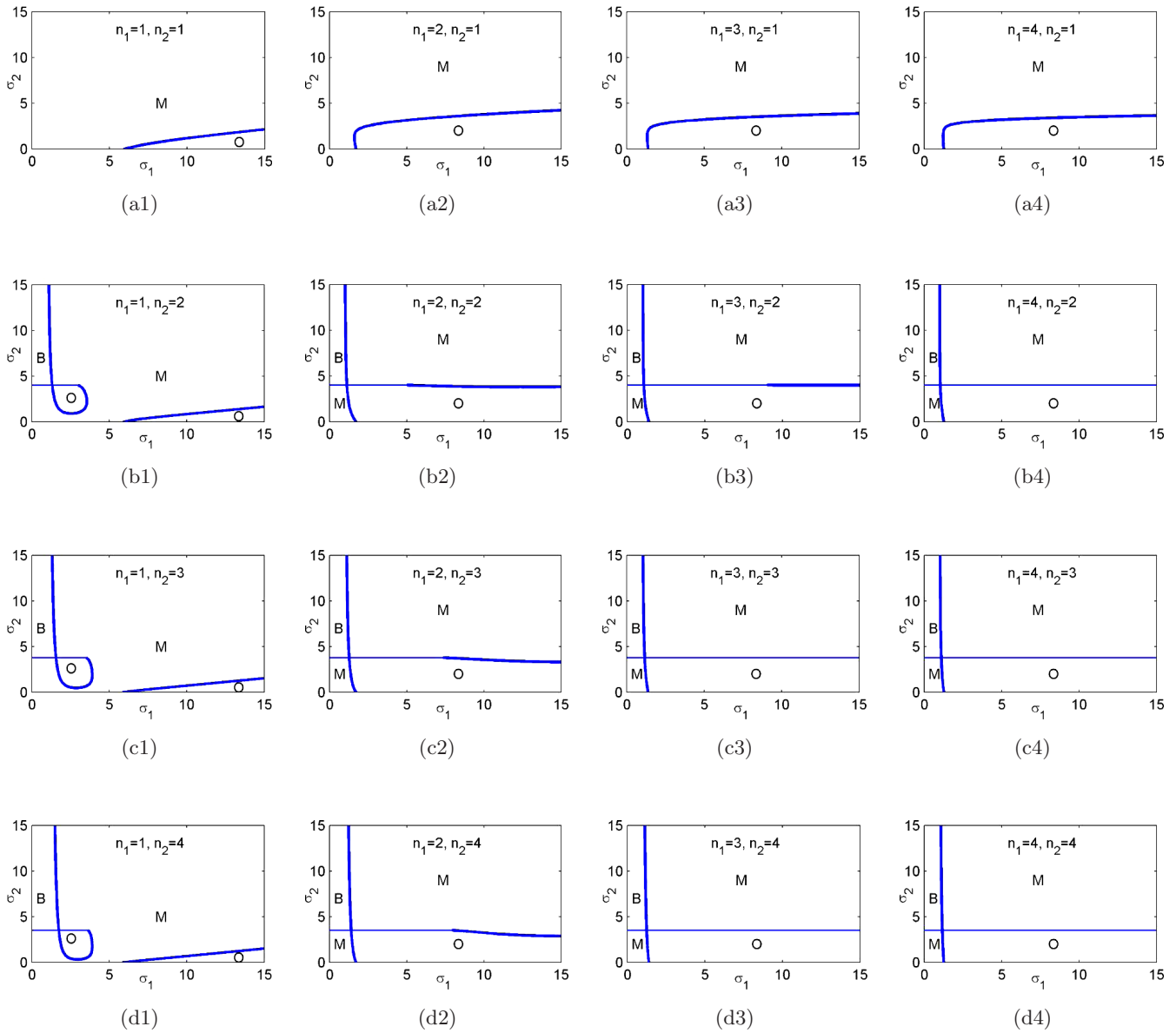

Fig. 5. Influence on the system behaviors with the synergistic effect (Hill coefficients). The abbreviations and symbols are the same as those in Fig. 4. The other parameters are $K = 2$, $\alpha_2 = 6$ and $\alpha_4 = 4$ in addition to the values of n_1 and n_2 marked in the diagram.

in σ_2, the system will also enter the subregion M2, making $X = 0$. With a weak auto-feedback strength (σ_1), of course, the positive regulation strength (σ_2) can also acquire a small value to stabilize the system, reducing the oscillation area. Additionally, when the auto-feedback strength (σ_1) is less than a certain threshold [the value is approximately 6 in Fig. 4(a1) and 1.6 in Fig. 4(a2)], the system is always in a stable state. It is noted that the bistability phenomenon is not observed when $n_2 = 1$, which indicates that a positive feedback loop is the only necessary condition to generate bistability and other conditions that must be satisfied to fully guarantee the bistability of a specific system.

Second, when $n_2 = 2$, the large auto-negative ratio (σ_1) easily induces an oscillation and the system can be stabilized by the suitable relative strength of the positive feedback (σ_2), which causes it to enter a stable subregion of M3 or M2 [Fig. 4(b)]. However, the system now exhibits bistability under the conditions of a small auto-negative ratio (σ_1) and a large relative strength of the positive feedback (σ_2) [Fig. 4(b1) or 4(b2)]. Because the auto-negative ratio is smaller ($\sigma_1 < 1$), the system

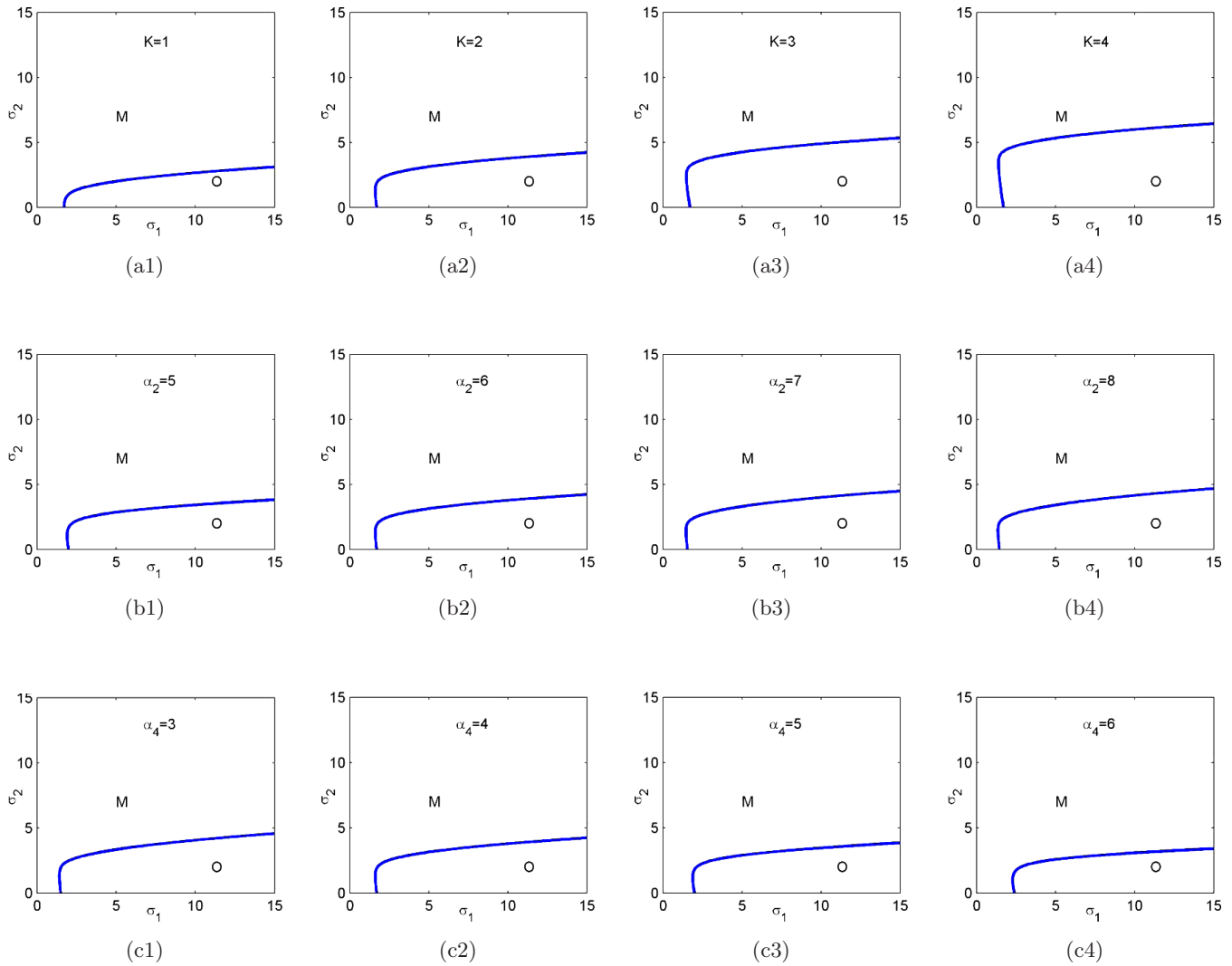

Fig. 6. The system dynamical behaviors about the perturbation of parameter K, α_2 or α_4 when $n_1 = 2$ and $n_2 = 1$. $K = 2$, $\alpha_2 = 6$ and $\alpha_4 = 4$, except for the values marked in the diagram. The abbreviations and symbols are the same as those in Fig. 4.

enters the subregion B1. With an increase in the auto-negative ratio ($\sigma_1 > 1$), the system enters the subregion B2 [Figs. 4(b1) and 4(b2)]. Figure 4 shows that B2 is narrower than B1. At the same time, it can be observed that the size of the bistable region can be adjusted by the relative strength of the positive feedback when the auto-negative ratio is fixed (the size is actually decreasing as σ_2 is increasing, but not significantly).

Third, we further analyze the effect of feedback on monostable and bistable states. We first fixed the relative strength of the positive feedback (σ_2): it is obvious that the weak relative strength of the positive feedback [$\sigma_2 \leq 4$, Figs. 4(b1) and 4(b2)] will not cause the system to have bistable performance. To observe bistable phenomena, we set $\sigma_2 = 4.1$. Therefore, the auto-negative ratio will determine whether the system is monostable or bistable (Fig. 9). When the auto-negative ratio is less than 1.314 [Fig. 9(a1)] or less than 1.14 [Fig. 9(b1)], the system exhibits rich bistable phenomena. When the auto-negative ratio is within domain $(0, 1)$, e.g. $\sigma_1 = 0.5$ [Figs. 9(a2) and 9(b2)], the system has two stable EPs, E_1 and E_{22}. At this time, although the system can switch between the two equilibrium states, X is equal to 0. If $\sigma_1 = 1.08$ [Figs. 9(a3) and 9(b3)], the system will switch between two stable equilibrium states, E_{22} and E_3, exhibiting bistability. The stability of the origin E_1 is inherited by the EP E_3. Because

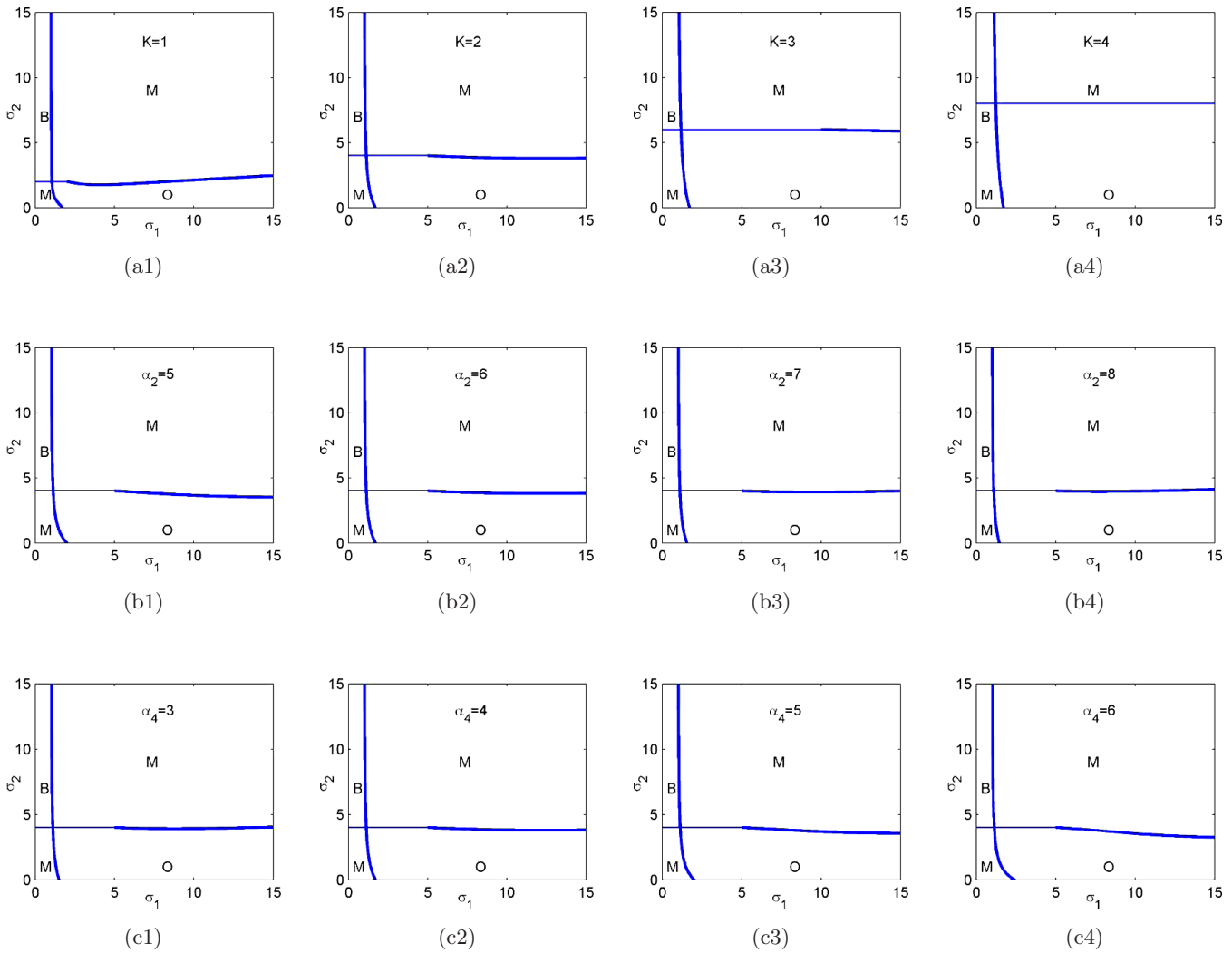

Fig. 7. The system dynamical behaviors about the perturbation of parameter K, α_2 or α_4 when $n_1 = 2$ and $n_2 = 2$. $K = 2$, $\alpha_2 = 6$ and $\alpha_4 = 4$, except for the values marked in the diagram. The abbreviations and symbols are the same as those in Fig. 4.

the auto-negative ratio increases continuously, the system will enter the monostable subregion M2, showing no bistable phenomenon [Fig. 4(b)].

Specifically, as the auto-negative ratio (σ_1) increases, the system will have a supercritical Hopf bifurcation when $n_1 = 2$ and $n_2 = 2$ [Fig. 9(b1)], showing a bistability phenomenon that is not easily observed [$\sigma_1 = 1.12$ in Fig. 10(b)], a stable equilibrium state and a stable limit cycle (the second type of bistability). However, this area is so small that only the second bistable type can be observed when the σ_1 belongs to a narrow interval (1.11, 1.14) [Fig. 9(b1)]. Therefore, we do not specifically describe the region in Fig. 4. As the auto-negative ratio increases when $n_1 = 1$ and $n_2 = 2$ [Fig. 9(a1)], the system transits from subregion B2 to subregion M2 and can have a subcritical Hopf bifurcation that produces an unstable limit cycle [Fig. 10(a)]. Similarly, the region is also very small and the phenomenon can be observed only when the σ_1 is in the interval (1.29, 1.314) [Fig. 9(a1)].

Finally, we consider the effect of the relative strength of the positive feedback (σ_2) on the bistability by fixing the auto-negative ratio (σ_1). From the above analysis, only when $n_2 = 2$ and the auto-negative ratio is small (such as $\sigma_1 < 1.314$ when $n_2 = 1$ or $\sigma_1 < 1.14$ when $n_2 = 2$), the bistable phenomenon can be observed if the relative strength of the positive feedback σ_2 is greater than 4. With an increase in the relative strength of the positive feedback, the whole bistable region slowly becomes smaller, while the bistable subregion B2

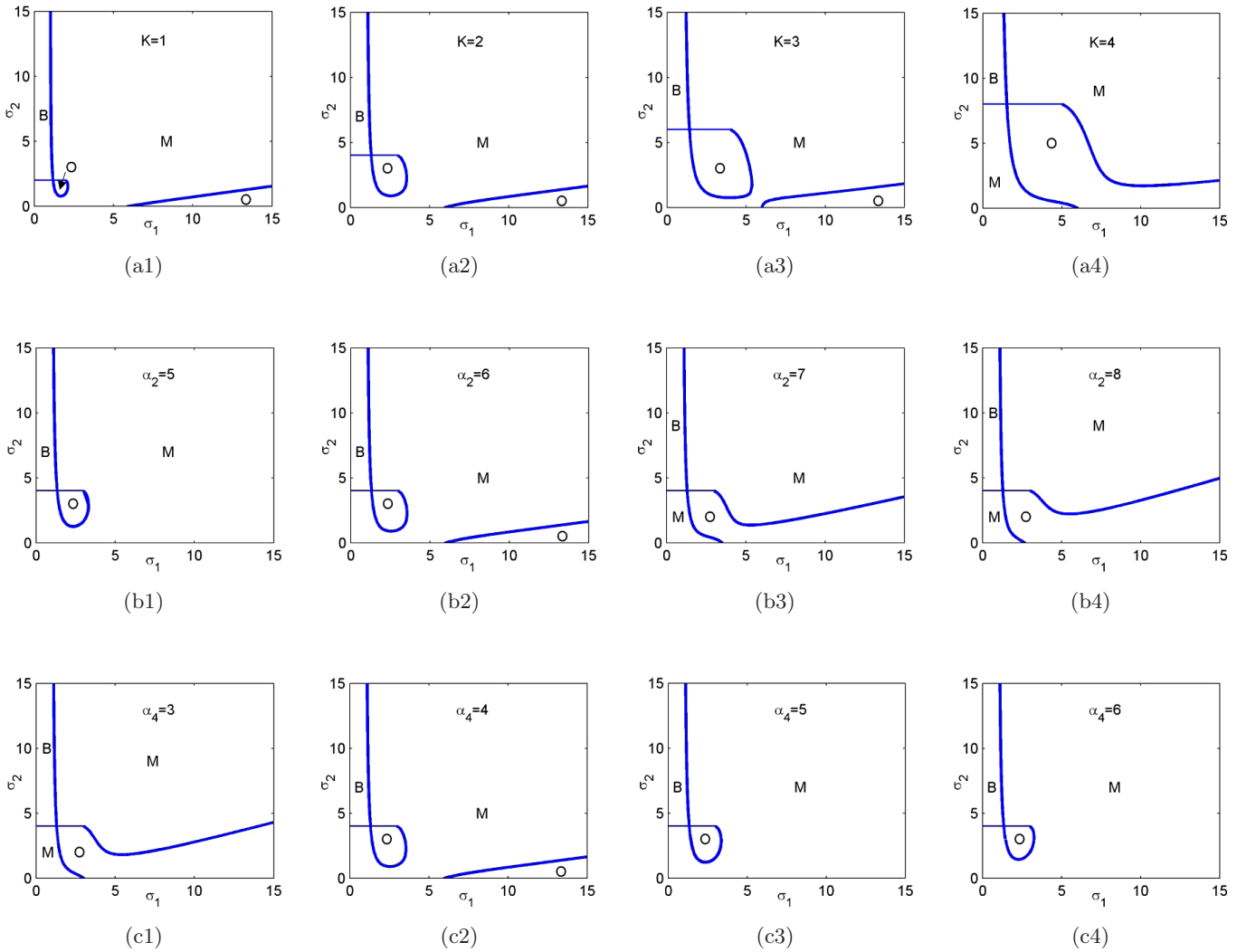

Fig. 8. The system dynamical behaviors about the perturbation of parameters K, α_2 or α_4 when $n_1 = 1$ and $n_2 = 2$. $K = 2$, $\alpha_2 = 6$ and $\alpha_4 = 4$, except for the values marked in the diagram. The abbreviations and symbols are the same as those in Fig. 4.

slowly becomes smaller, the bistable subregion B1 remains unchanged ($\sigma_1 < 1$) [Figs. 4(b1) and 4(b2)].

4.2.2. *Oscillations*

An oscillation is a basic and important property that is exhibited by many regulatory systems and is a common phenomenon in life processes, for example, the circadian rhythm and the cell cycle. Therefore, it is very important to master the oscillation-generating mechanism for understanding biological regulatory networks. We investigate how the cooperation of positive and negative feedback induces an oscillation. For the sake of convenience, we change only the strength of the two feedbacks and discuss their effect on the oscillation interval, period and amplitude when the other parameters are unchanged.

First, we analyze the impact of parameter σ_1 by fixing the relative positive feedback strength σ_2 in the two cases, i.e. one strong strength [$\sigma_2 = 3.8$ in Figs. 11(a1) and 11(a2)] and one weak strength [$\sigma_2 = 0.8$ in Figs. 11(b1) and 11(b2)]. When σ_2 is large and $\sigma_2 = 3.8$, the system will have a subcritical Hopf bifurcation at $\sigma_1 \approx 1.32$ and $\sigma_1 \approx 3.2$ [Figs. 11(a1) and 12] or $\sigma_1 \approx 1.12$ [Fig. 11(a2)], due to σ_1 gradually being increased, which results in an unstable limit cycle (this region is very small and difficult to observe) in a stable subregion M3 in Fig. 4(b) regardless of whether $n_1 = 1$ or 2. Then, the system quickly enters the stable limit cycle region, exhibiting a periodic oscillation, and

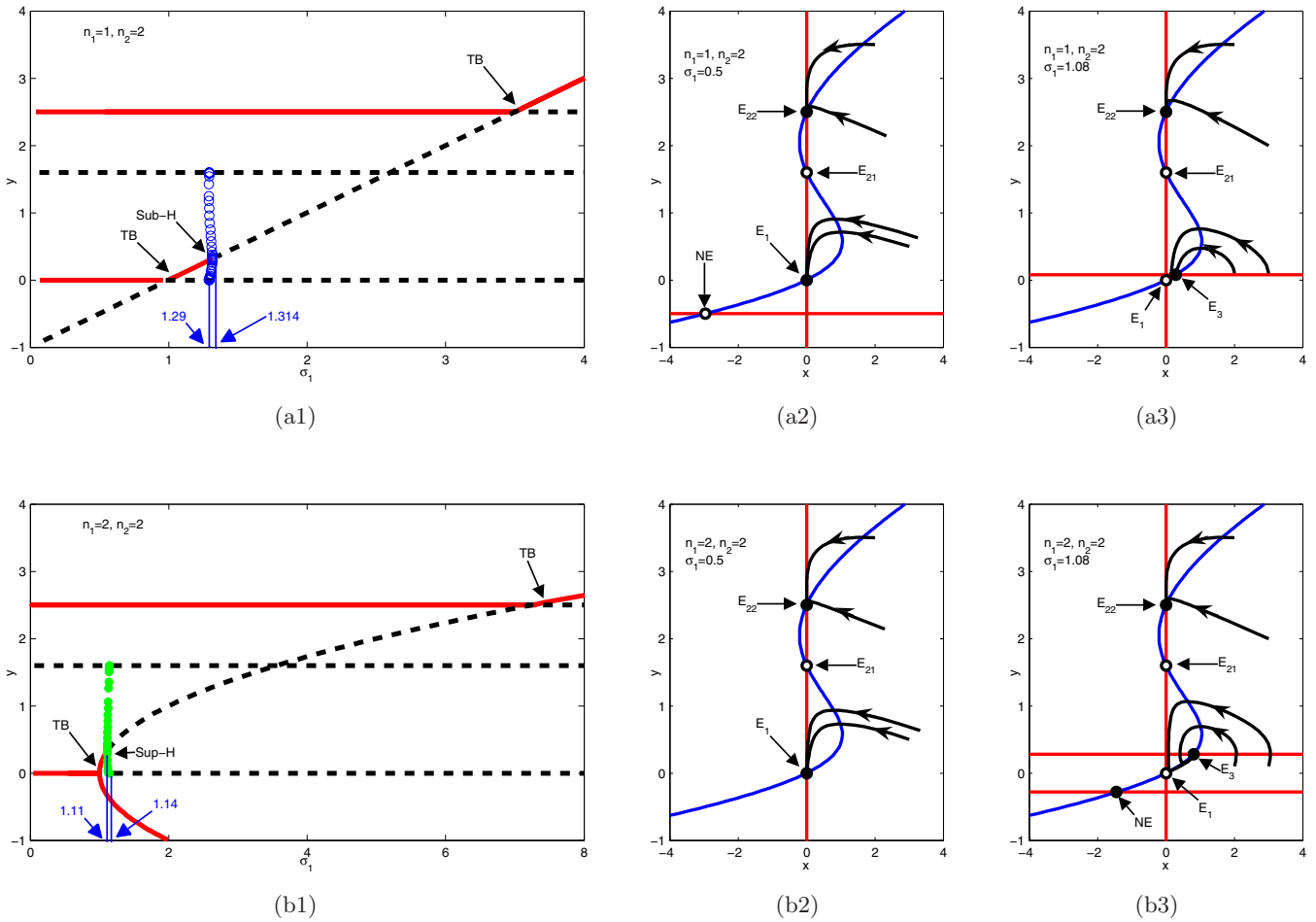

Fig. 9. Bifurcation diagrams about σ_1 and bistable phase diagrams about x–y. (a1) is the bifurcation diagram about σ_1 when $n_1 = 1$. (a2) and (a3) are (a1)'s phase diagrams about x–y when $\sigma_1 = 0.5$ or $\sigma_1 = 1.08$, respectively. (b1) is the bifurcation diagram about σ_1 when $n_1 = 2$. (b2) and (b3) are (b1)'s phase diagrams about x–y when $\sigma_1 = 0.5$ or $\sigma_1 = 1.08$, respectively. Blue hollow circles and green solid circles in bifurcation diagrams represent the maximum and minimum amplitudes of unstable or stable limit cycles, respectively. Red solid lines and black dashed lines in bifurcation diagrams indicate stable or unstable equilibrium points, respectively. Red solid lines and blue solid lines in phase diagrams are x-nullcline or y-nullcline, respectively. Their intersections are equilibrium points, of which solid or hollow circles are stable or unstable, respectively. E_1, E_{21}, E_{22} and E_3 are all non-negative equilibrium points discussed in Theorem 2 and NE is the negative equilibrium point which is not considered in this study. Black solid curves with arrows in phase diagrams refer to sample trajectories. The other abbreviations and symbols are the same as in Fig. 4. The other parameters are $\sigma_2 = 4.1$, $K = 2$, $\alpha_2 = 6$ and $\alpha_4 = 4$ in addition to the value of σ_1, n_1 and n_2 marked in the diagrams.

re-enters the stable region M3 when $\sigma_1 \approx 3.42$ [in Fig. 11(a1)] or $\sigma_1 \approx 10.86$ [in Fig. 11(a2)]. From Fig. 12, if σ_1 belongs to the interval (3.2, 3.42), the system has two limit cycles simultaneously, and they tend to coalesce at $\sigma_1 \approx 3.42$, forming a saddle-node bifurcation on a periodic orbit (SN-PO). However, with the continued increase in σ_1, the system will again have a Hopf bifurcation [supercritical bifurcation at $\sigma_1 \approx 28.3$ in Fig. 11(a1) or $\sigma_1 \approx 13.98$ in Fig. 11(a2)], re-entering the oscillation region. The subgraphs in Fig. 11(a) describe the dependencies of the system's period on the feedback strength σ_1. With an increase in σ_1, the period first reduces and then stays almost constant.

When the relative strength of the positive feedback σ_2 is small ($\sigma_2 = 0.8$), the oscillation is relatively simple [Figs. 11(b1) and 11(b2)]. The system will undergo supercritical Hopf bifurcation, resulting in a stable limit cycle, in the subregion M3 with an increase of σ_1. The system enters an oscillation region and is no longer back to the stable region M3 from the oscillation region, and the period of the system stays almost constant [Fig. 11(b)]. From Fig. 11(a), when $\sigma_2 = 3.8$, the oscillation amplitude

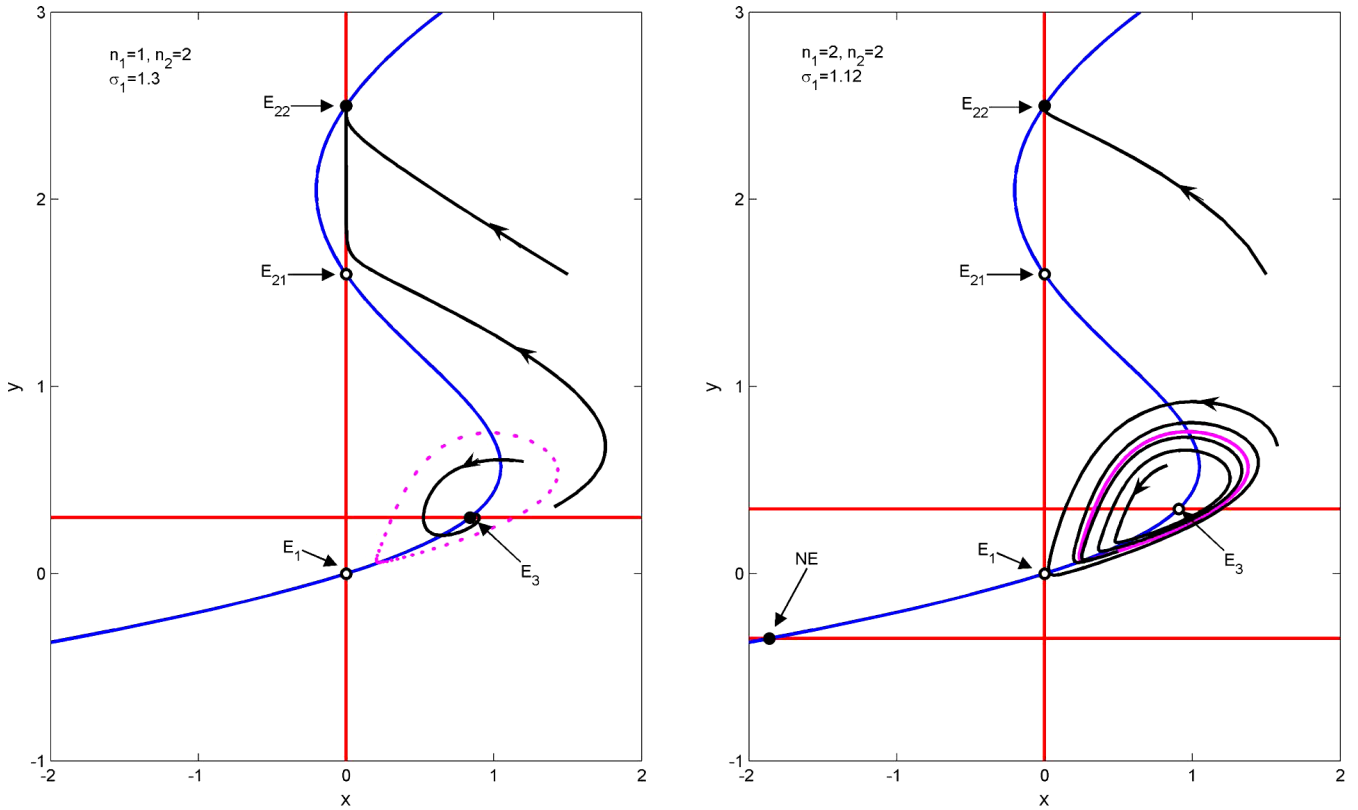

Fig. 10. Bistable phase diagrams about x–y. (a) is a phase diagram about x–y when $\sigma_1 = 1.3$ and $n_1 = 1$. (b) is a phase diagram about x–y when $\sigma_1 = 1.12$ and $n_1 = 2$. The red solid lines and blue solid lines are x-nullcline or y-nullcline, respectively. Their intersections are equilibrium points, of which solid or hollow circles are stable or unstable, respectively. Black solid curves with arrows refer to sample trajectories. Magenta dashed or solid lines represent unstable or stable limit cycles, respectively. The abbreviations and symbols are the same as those in Fig. 9. The other parameters are $\sigma_2 = 4.1$, $K = 2$, $\alpha_2 = 6$ and $\alpha_4 = 4$ in addition to the value of σ_1, n_1 and n_2 marked in the diagrams.

initially increases and then decreases to 0 in the oscillation range (1.32, 3.42) [Fig. 11(a1)] or (1.12, 10.86) [Fig. 11(a2)], with an increase in σ_1. In the oscillation region (28.3, 30) [Fig. 11(a1)] or (13.98, 30) [Fig. 11(a2)], as the value of σ_1 is increased, the amplitude of the oscillation is a monotonically increasing function of σ_1. When $\sigma_2 = 0.8$ [Fig. 11(b)], the amplitude will become increasingly large after the system enters the oscillation region, similar to the second case in Fig. 11(a).

Second, we examine the impact of the parameter σ_2 on the oscillation (Fig. 13). When $\sigma_1 = 1.4$, the system will undergo Hopf bifurcation [subcritical Hopf bifurcation in Fig. 13(a1) and supercritical Hopf bifurcation in Fig. 13(a2)] in the stable subregion M3 as the relative strength σ_2 increases. Then, the system undergoes a saddle-node bifurcation (SNB) and enters a stable subregion M2. In the oscillation region, the period and amplitude are increased with an increase in σ_2, and the system period increases exponentially. When $\sigma_1 = 8$, the system will be back in the stable region from an oscillation region with an increase in σ_2 [Fig. 13(b)], which indicates that the positive feedback can stabilize the system. In the oscillation region, the system's period and amplitude decrease as the parameter σ_2 increases when $n_1 = 1$, while the period and amplitude increase slowly at the beginning and then decrease suddenly when $n_1 = 2$, which shows different behaviors.

These results indicate that the strength of the positive and negative feedback must be within a certain range to induce an oscillation. Furthermore, the period and amplitude are nonlinear functions of the two feedback strengths, especially the strength of positive feedback, which mainly adjusts the period

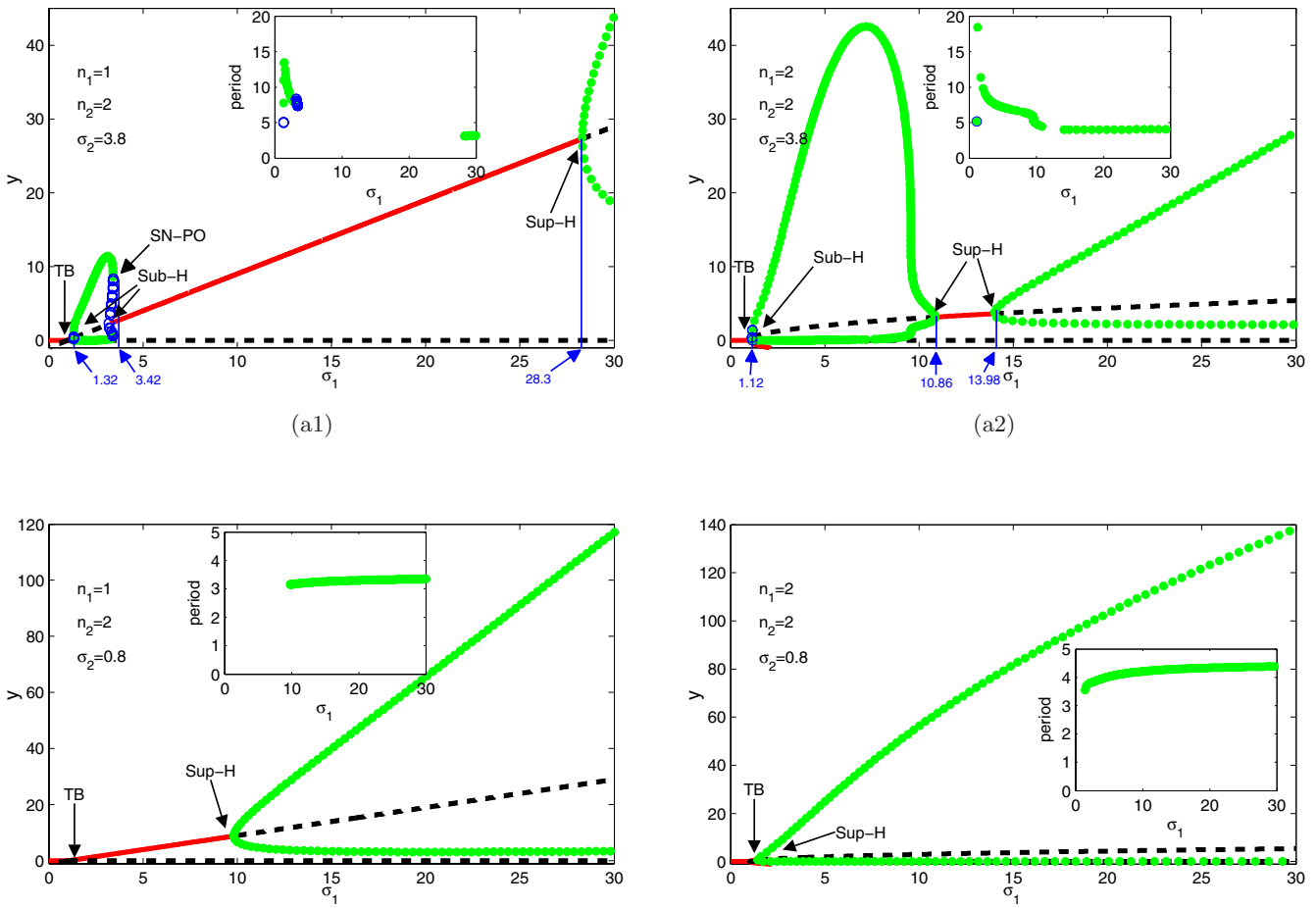

Fig. 11. Hopf bifurcation diagrams with a continual oscillation about σ_1 and a period about σ_1 in the subdiagrams. The blue hollow circles and green solid circles in the bifurcation diagrams represent the maximum and minimum amplitudes of the unstable or stable limit cycle, respectively. The red solid lines and black dashed lines in the bifurcation diagrams indicate stable or unstable equilibrium points, respectively. SN-PO denotes a saddle-node bifurcation point in a periodic orbit. The other abbreviations and symbols are the same as those in Fig. 9. The other parameters are $K = 2$, $\alpha_2 = 6$ and $\alpha_4 = 4$ in addition to the value of σ_2, n_1 and n_2 marked in the diagrams.

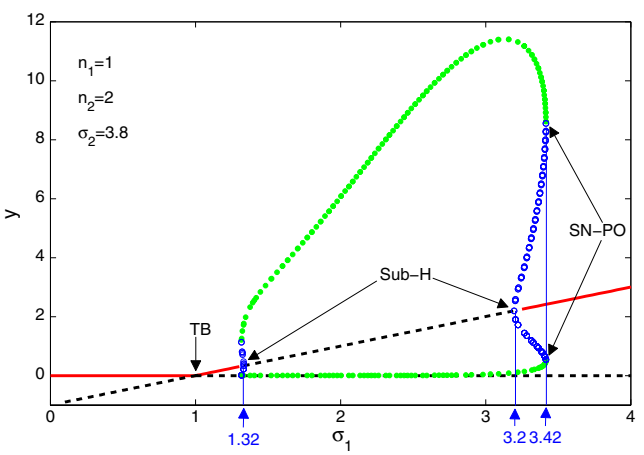

Fig. 12. A local enlarged diagram of Fig. 11(a1).

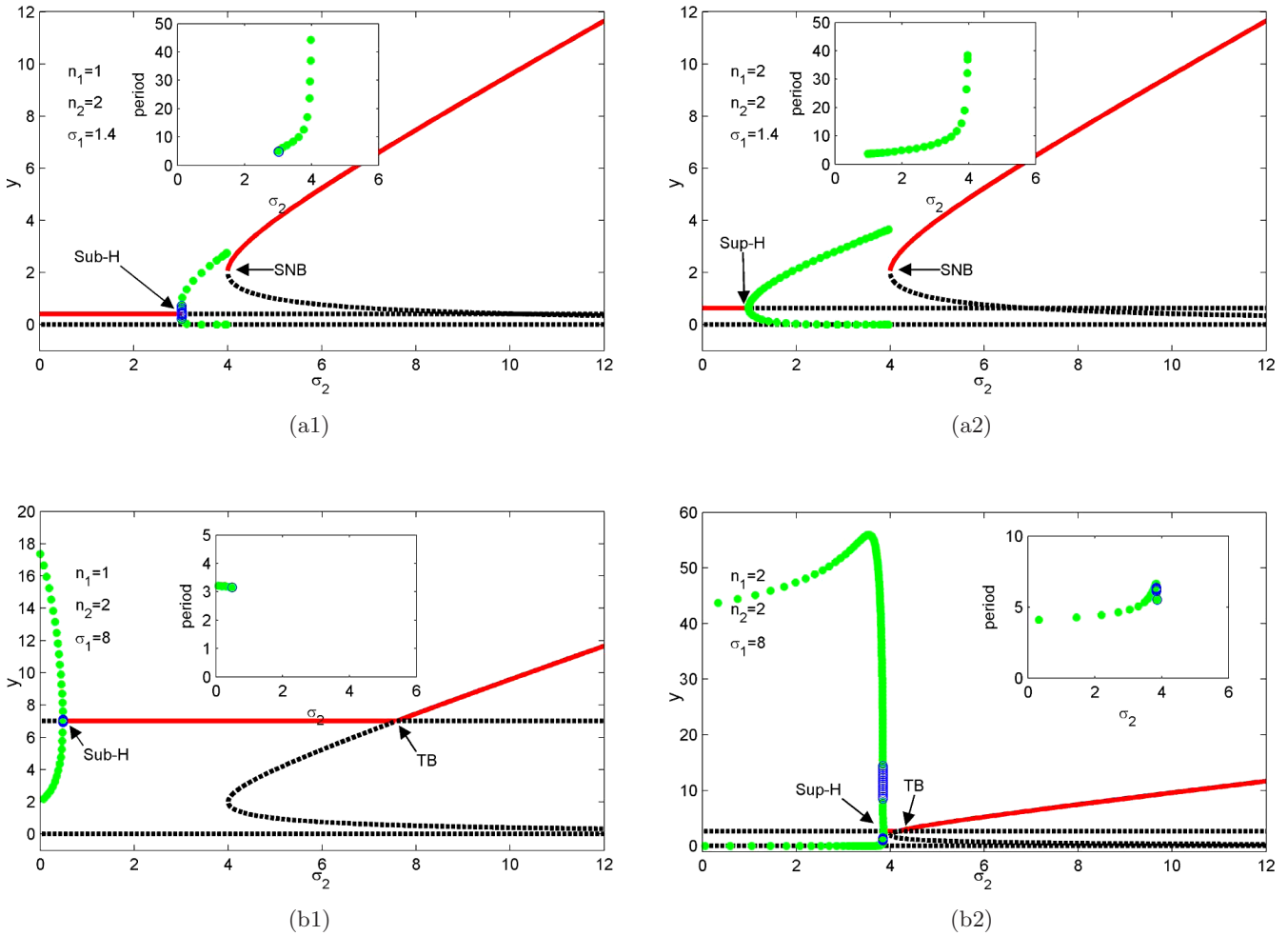

Fig. 13. Hopf bifurcation diagrams with continual oscillation about σ_2 and a period of approximately σ_2 in the subdiagrams. Blue hollow circles and green solid circles in the bifurcation diagrams represent the maximum and minimum amplitudes of an unstable or stable limit cycle, respectively. The red solid lines and black dashed lines in the bifurcation diagrams indicate stable or unstable equilibrium points, respectively. The abbreviations and symbols are the same as those in Fig. 9. The other parameters are $K = 2$, $\alpha_2 = 6$ and $\alpha_4 = 4$, in addition to the values of σ_1, n_1 and n_2 marked in the diagrams.

of the oscillation, and the strength of the auto-negative feedback mainly adjusts the amplitude of the oscillation.

5. Conclusions

In this study, we investigate the complex dynamical behaviors of a coupled network that is composed of one negative feedback, one auto-feedback (self-replication) and one positive feedback, which are derived from innate immune responses. The main contributions of this study include three aspects.

First, we theoretically infer the conditions under which the network has the stable equilibrium points (EPs) and find that no more than three stable non-negative EPs exist in this network for all of the cases. Furthermore, we determine that the necessary condition for the production of bistability is that the Hill coefficient of the positive feedback loop is greater than or equal to 2.

Second, through global and local bifurcation analysis, we reveal that the relative strengths of the auto-feedback, negative and positive feedback are important quantities for inducing various distinguishable dynamical behaviors. Furthermore, we find that the relative activation coefficient K and the relative degradation ratios α_2 and α_4 have no obvious influence on the network's dynamical behaviors.

Third, the strength of the positive and negative feedbacks must be within a certain range to induce oscillations. From the numerical simulations, we also find that the strength of the positive feedback can adjust the period of oscillation and that the

strength of the auto-negative feedback can adjust the amplitude of the oscillation.

These findings provide new insights into the dynamical behaviors of complex networks that interlink positive and negative feedback loops. This work also contributes to our systems-level understanding of molecular mechanisms in modularized networks.

Acknowledgments

The authors thank the anonymous reviewers for their helpful comments and suggestions. This work was supported by the Chinese National Natural Science Foundation (No. 61173060), the Major Research Plan of the National Natural Science Foundation of China (No. 91230118).

References

Alon, U. [2006] *Introduction to Systems Biology*: *Design Principles of Biological Circuits* (CRC Press, Boca Raton).

Andrianantoandro, E., Basu, S., Karig, D. K. & Weiss, R. [2006] "Synthetic biology: New engineering rules for an emerging discipline," *Mol. Syst. Biol.* **2**, 0028.

Cinquin, O. & Demongeot, J. [2002] "Positive and negative feedback: Striking a balance between necessary antagonists," *J. Theor. Biol.* **216**, 229–241.

Dorf, R. C. & Bishop, R. H. [2001] *Modern Control Systems*, 9th edition (Prentice Hall Press).

Elowitz, M. B. & Leibler, S. [2000] "A synthetic oscillatory network of transcriptional regulators," *Nature* **403**, 335–338.

Endy, D. [2005] "Foundations for engineering biology," *Nature* **438**, 449–453.

Ermentrout, B. [2002] *Simulating, Analyzing, and Animating Dynamical Systems*: *A Guide to XPPAUT for Researchers and Students* (SIAM, Philadelphia).

Ferrell, J. E. [2002] "Self-perpetuating states in signal transduction: Positive feedback, double-negative feedback and bistability," *Curr. Opin. Cell Biol.* **14**, 140–148.

Gardner, T., Cantor, C. & Collins, J. [2000] "Construction of a genetic toggle switch in *Escherichia coli*," *Nature* **403**, 339–342.

Guantes, R. & Poyatos, J. [2006] "Dynamical principles of two-component genetic oscillators," *PLoS Comput. Biol.* **2**, 0188–0197.

Hale, J. [1977] *Theory of Functional Differential Equations* (Springer-Verlag, NY).

Haseloff, J. & Ajioka, J. [2009] "Synthetic biology: History, challenges and prospects," *J. R. Soc. Interf.* **6**, S389–S391.

Iranfar, N., Fuller, D. & Loomis, W. [2006] "Transcriptional regulation of post-aggregation genes in *Dictyostelium* by a feed-forward loop involving GBF and LagC," *Dev. Biol.* **290**, 460–469.

Kuznetsov, Y. A. [1998] *Elements of Applied Bifurcation Theory*, 2nd edition (Springer-Verlag, NY).

Liu, X. L. & Liu, S. Q. [2012] "Codimension-two bifurcation analysis in two-dimensional Hindmarsh–Rose model," *Nonlin. Dyn.* **67**, 847–857.

McMillen, D., Kopell, N., Hasty, J. & Collins, J. J. [2002] "Synchronizing genetic relaxation oscillators by intercell signaling," *Proc. Natl. Acad. Sci.* **99**, 679–684.

Milo, R., Shen-Orr, S., Itzkovitz, S., Kashtan, N., Chklovskii, D. & Alon, U. [2002] "Network motifs: Simple building blocks of complex networks," *Science* **298**, 824–827.

Novák, B. & Tyson, J. J. [2008] "Design principles of biochemical oscillators," *Nat. Rev. Mol. Cell Biol.* **9**, 981–991.

Pfeuty, B. & Kaneko, K. [2009] "The combination of positive and negative feedback loops confers exquisite flexibility to biochemical switches," *Phys. Biol.* **6**, 046013.

Pomerening, J. R., Kim, S. Y. & Ferrell, J. E. [2005] "Systems-level dissection of the cell-cycle oscillator: Bypassing positive feedback produces damped oscillations," *Cell* **122**, 565–578.

Qiu, H. H. & Zhou, T. S. [2012] "Feedback-induced complex dynamics in a two-component regulatory circuit," *Int. J. Bifurcation and Chaos* **22**, 1250059.

Serrano, L. [2007] "Synthetic biology: Promises and challenges," *Mol. Syst. Biol.* **3**, 158.

Shen-Orr, S., Milo, R., Mangan, S. & Alon, U. [2002] "Network motifs in the transcriptional regulation network of *Escherichia coli*," *Nat. Genet.* **31**, 64–68.

Snoussi, E. H. [1998] "Necessary conditions for multistationarity and stable periodicity," *J. Biol. Syst.* **6**, 3–9.

Song, H., Smolen, P., Av-Ron, E., Baxter, D. A. & Byrne, J. H. [2007] "Dynamics of a minimal model of interlocked positive and negative feedback loops of transcriptional regulation by cAMPresponse element binding proteins," *Biophys. J.* **92**, 3407–3424.

Stricker, J., Cookson, S., Bennett, M. R., Mather, W. H., Tsimring, L. S. & Hasty, J. [2008] "A fast, robust and tunable synthetic gene oscillator," *Nature* **456**, 516–519.

Süel, G. M., Garcia-Ojalvo, J., Liberman, L. M. & Elowitz, M. B. [2006] "An excitable gene regulatory circuit induces transient cellular differentiation," *Nature* **440**, 545–550.

Tan, J. Y., Pan, R. G., Qiao, L., Zou, X. F. & Pan, Z. S. [2012] "Modeling and dynamical analysis of virus-triggered innate immune signaling pathways," *PLoS ONE* **7**, e48114.

Thomas, R. [1994] "The role of feedback circuits: Positive feedback circuits are a necessary condition for positive real eigenvalues of the Jacobian matrix," *Berichte Der Bunsengesellschaft* **98**, 1148–1151.

Tian, X. J., Zhang, X. P., Liu, F. & Wang, W. [2009] "Interlinking positive and negative feedback loops creates a tunable motif in gene regulatory networks," *Phys. Rev. E* **80**, 011926.

Tsai, T. Y. C., Choi, Y. S., Ma, W. Z., Pomerening, J. R., Tang, C. & Ferrell, J. E. [2008] "Robust, tunable biological oscillations from interlinked positive and negative feedback loops," *Science* **321**, 126–129.

Zhang, J. J., Yuan, Z. J., Li, H. X. & Zhou, T. S. [2010] "Architecture-dependent robustness and bistability in a class of genetic circuits," *Biophys. J.* **99**, 1034–1042.

Appendix A

Proof [Proof of Theorem 1]

(1) The Jacobi matrix of system (3) at $E_1^{n_1,1}$ is

$$J_{E_1^{n_1,1}} = \begin{pmatrix} (\sigma_1 - 1)\alpha_2 & 0 & 0 \\ 1 & \left(\frac{\sigma_2}{K} - 1\right)\alpha_4 & 0 \\ 0 & 1 & -1 \end{pmatrix}.$$

Its corresponding characteristic equation is

$$|\lambda I - J_{E_1^{n_1,1}}| = \begin{vmatrix} \lambda - (\sigma_1 - 1)\alpha_2 & 0 & 0 \\ -1 & \lambda - \left(\frac{\sigma_2}{K} - 1\right)\alpha_4 & 0 \\ 0 & -1 & \lambda + 1 \end{vmatrix}$$

$$= [\lambda - (\sigma_1 - 1)\alpha_2]\left[\lambda - \left(\frac{\sigma_2}{K} - 1\right)\alpha_4\right](\lambda + 1) = 0.$$

We can see from the above equation that its roots have negative real parts when $\sigma_1 < 1$ and $\sigma_2 < K$, which shows that the system (3) is locally asymptotically stable at $E_1^{n_1,1}$.

(2) The Jacobi matrix of system (3) at $E_2^{n_2,1}$ is

$$J_{E_2^{n_1,1}} = \begin{pmatrix} \frac{\sigma_1\alpha_2}{1 + (\overline{z}_2^{n_1,1})^{n_1}} - \alpha_2 & 0 & 0 \\ 1 & \frac{K\sigma_2\alpha_4}{(K + \overline{y}_2^{n_1,1})^2} - \alpha_4 & 0 \\ 0 & 1 & -1 \end{pmatrix}.$$

Its corresponding characteristic equation is

$$|\lambda I - J_{E_2^{n_1,1}}| = \begin{vmatrix} \lambda + \alpha_2 - \frac{\sigma_1\alpha_2}{1 + (\overline{z}_2^{n_1,1})^{n_1}} & 0 & 0 \\ -1 & \lambda + \alpha_4 - \frac{K\sigma_2\alpha_4}{(K + \overline{y}_2^{n_1,1})^2} & 0 \\ 0 & -1 & \lambda + 1 \end{vmatrix}$$

$$= \left[\lambda + \alpha_2 - \frac{\sigma_1\alpha_2}{1 + (\overline{z}_2^{n_1,1})^{n_1}}\right]\left[\lambda + \alpha_4 - \frac{K\sigma_2\alpha_4}{(K + \overline{y}_2^{n_1,1})^2}\right](\lambda + 1)$$

$$= \left[\lambda + \alpha_2 - \frac{\sigma_1\alpha_2}{1 + (\sigma_2 - K)^{n_1}}\right]\left(\lambda + \alpha_4 - \frac{K\alpha_4}{\sigma_2}\right)(\lambda + 1) = 0.$$

We can see from the above equation that its roots have negative real parts if $\sigma_2 > \max\{K, K + (\sigma_1 - 1)^{\frac{1}{n_1}}\}$, which shows that the system (3) is locally asymptotically stable at $E_2^{n_2,1}$.

(3) The Jacobi matrix of system (3) at $E_3^{n_2,1}$ is

$$J_{E_3^{n_1,1}} = \begin{pmatrix} \dfrac{\sigma_1\alpha_2}{1+(\overline{z}_3^{n_1,1})^{n_1}} - \alpha_2 & 0 & -\dfrac{n_1\sigma_1\alpha_2\overline{x}_3^{n_1,1}(\overline{z}_3^{n_1,1})^{n_1-1}}{[1+(\overline{z}_3^{n_1,1})^{n_1}]^2} \\ 1 & \dfrac{K\sigma_2\alpha_4}{(K+\overline{y}_3^{n_1,1})^2} - \alpha_4 & 0 \\ 0 & 1 & -1 \end{pmatrix}.$$

Its corresponding characteristic equation is

$$|\lambda I - J_{E_3^{n_1,1}}| = \begin{vmatrix} \lambda + \alpha_2 - \dfrac{\sigma_1\alpha_2}{1+(\overline{z}_3^{n_1,1})^{n_1}} & 0 & \dfrac{n_1\sigma_1\alpha_2\overline{x}_3^{n_1,1}(\overline{z}_3^{n_1,1})^{n_1-1}}{[1+(\overline{z}_3^{n_1,1})^{n_1}]^2} \\ -1 & \lambda + \alpha_4 - \dfrac{K\sigma_2\alpha_4}{(K+\overline{y}_3^{n_1,1})^2} & 0 \\ 0 & -1 & \lambda + 1 \end{vmatrix}$$

$$= \left[\lambda + \alpha_2 - \frac{\sigma_1\alpha_2}{1+(\overline{z}_3^{n_1,1})^{n_1}}\right]\left[\lambda + \alpha_4 - \frac{K\sigma_2\alpha_4}{(K+\overline{y}_3^{n_1,1})^2}\right](\lambda+1) + \frac{n_1\sigma_1\alpha_2\overline{x}_3^{n_1,1}(\overline{z}_3^{n_1,1})^{n_1-1}}{[1+(\overline{z}_3^{n_1,1})^{n_1}]^2}$$

$$= \lambda(\lambda+1)\left\{\lambda + \alpha_4 - \frac{K\sigma_2\alpha_4}{\left[K+(\sigma_1-1)^{\frac{1}{n_1}}\right]^2}\right\} + \frac{n_1\alpha_2\alpha_4(\sigma_1-1)\left[K+(\sigma_1-1)^{\frac{1}{n_1}} - \sigma_2\right]}{\sigma_1\left[K+(\sigma_1-1)^{\frac{1}{n_1}}\right]} = 0,$$

i.e.

$$\lambda^3 + \left[1 + \alpha_4 - \frac{K\sigma_2\alpha_4}{\left[K+(\sigma_1-1)^{\frac{1}{n_1}}\right]^2}\right]\lambda^2 + \left[\alpha_4 - \frac{K\sigma_2\alpha_4}{\left[K+(\sigma_1-1)^{\frac{1}{n_1}}\right]^2}\right]\lambda + \frac{n_1\alpha_2\alpha_4(\sigma_1-1)\left[K+(\sigma_1-1)^{\frac{1}{n_1}} - \sigma_2\right]}{\sigma_1\left[K+(\sigma_1-1)^{\frac{1}{n_1}}\right]} = 0. \tag{A.1}$$

When $\sigma_1 > 1$, $\sigma_2 < K + (\sigma_1 - 1)^{\frac{1}{n_1}}$ and $\alpha_2 < C^{n_1,1}$, we can deduce that all coefficients of Eq. (A.1) are positive and the following inequality holds:

$$\left[1 + \alpha_4 - \frac{K\sigma_2\alpha_4}{\left[K+(\sigma_1-1)^{\frac{1}{n_1}}\right]^2}\right]\left[1 - \frac{K\sigma_2}{\left[K+(\sigma_1-1)^{\frac{1}{n_1}}\right]^2}\right] > \frac{n_1\alpha_2(\sigma_1-1)\left[K+(\sigma_1-1)^{\frac{1}{n_1}} - \sigma_2\right]}{\sigma_1\left[K+(\sigma_1-1)^{\frac{1}{n_1}}\right]}.$$

Thus, all conditions in Routh–Hurwitz criterion are satisfied, accordingly, all roots of Eq. (A.1) have negative real parts, which shows that the system (3) is locally asymptotically stable at $E_3^{n_2,1}$. ■

Appendix B

Proof [Proof of Lemma 1]. To facilitate the discussion below, the characteristic equation about EP $E_3^{n_1,n_2}$ ($n_2 = 1$ or 2) is denoted by

$$\lambda^3 + P\lambda^2 + Q\lambda + R = 0, \tag{B.1}$$

where

$$P = 1 + \alpha_4 - \frac{n_2\sigma_2\alpha_4 K^{n_2}(\sigma_1-1)^{\frac{n_2-1}{n_1}}}{\left[K^{n_2}+(\sigma_1-1)^{\frac{n_2}{n_1}}\right]^2}, \quad Q = \alpha_4 - \frac{n_2\sigma_2\alpha_4 K^{n_2}(\sigma_1-1)^{\frac{n_2-1}{n_1}}}{\left[K^{n_2}+(\sigma_1-1)^{\frac{n_2}{n_1}}\right]^2}$$

and

$$R = \frac{n_1\alpha_2\alpha_4(\sigma_1-1)\left[K^{n_2}+(\sigma_1-1)^{\frac{n_2}{n_1}} - \sigma_2(\sigma_1-1)^{\frac{n_2-1}{n_1}}\right]}{\sigma_1\left[K^{n_2}+(\sigma_1-1)^{\frac{n_2}{n_1}}\right]}.$$

According to the Hopf bifurcation theorem and the Routh–Hurwitz criteria, a Hopf bifurcation occurs at the following conditions $P > 0$, $Q > 0$, $R > 0$ and $PQ - R = 0$. Let

$$H(\lambda(\alpha_2), \alpha_2) = \lambda^3 + P\lambda^2 + Q\lambda + R. \quad \text{(B.2)}$$

The eigenvalues of Eq. (B.1) at $\alpha_2 = C^{n_1,n_2}$ are $\lambda_{1,2} = \pm i\sqrt{Q}$ and $\lambda_3 = -P < 0$.

To illustrate the Hopf bifurcation of the system at $\alpha_2 = C^{n_1,n_2}$, we need to prove $\mathrm{Re}(\frac{d\lambda_{1,2}(C^{n_1,n_2})}{d\alpha_2}) > 0$. Differentiating (B.2) yields

$$\frac{d\lambda}{d\alpha_2} = -\frac{\frac{\partial H}{\partial \alpha_2}}{\frac{\partial H}{\partial \lambda}} = -\frac{P'\lambda^2 + Q'\lambda + R'}{3\lambda^2 + 2P\lambda + Q},$$

where $P' = \frac{dP}{d\alpha_2} = 0$, $Q' = \frac{dQ}{d\alpha_2} = 0$ and $R' = \frac{dR}{d\alpha_2} = \frac{n_1\alpha_4(\sigma_1-1)\left[K^{n_2}+(\sigma_1-1)^{\frac{n_2}{n_1}} - \sigma_2(\sigma_1-1)^{\frac{n_2-1}{n_1}}\right]}{\sigma_1\left[K^{n_2}+(\sigma_1-1)^{\frac{n_2}{n_1}}\right]} > 0$.

The complex eigenvalues of Eq. (B.1), λ_1 and λ_2, occur in pairs. Thus, λ_1 is only used to calculate the following

$$\frac{d\lambda_1}{d\alpha_2} = -\frac{\frac{\partial H}{\partial \alpha_2}}{\frac{\partial H}{\partial \lambda_1}} = \frac{2QR' + 2P\sqrt{Q}R'i}{4Q^2 + 4P^2Q}.$$

We find the real part of the above equation (due to $\overline{x}_3^{n_1,n_2} > 0$)

$$\begin{aligned}\mathrm{Re}\left(\frac{d\lambda_1(C^{n_1,n_2})}{d\alpha_2}\right) &= \frac{2QR'}{4Q^2+4P^2Q} \\ &= \frac{2Q}{4Q^2+4P^2Q}\frac{n_1\alpha_4(\sigma_1-1)\left[K^{n_2}+(\sigma_1-1)^{\frac{n_2}{n_1}} - \sigma_2(\sigma_1-1)^{\frac{n_2-1}{n_1}}\right]}{\sigma_1\left[K^{n_2}+(\sigma_1-1)^{\frac{n_2}{n_1}}\right]} \\ &> 0.\end{aligned}$$

Therefore, a Hopf bifurcation occurs as α_2 passes through C^{n_1,n_2} for the system (2). ■

Appendix C

Proof [Proof of Theorem 3]

(1) The Jacobi matrix at $E_1^{n_1,n_2}$ ($\overline{x}_1^{n_1,n_2} = \overline{y}_1^{n_1,n_2} = \overline{z}_1^{n_1,n_2} = 0$) is

$$J_{E_1^{n_1,n_2}} = \begin{pmatrix} (\sigma_1-1)\alpha_2 & 0 & 0 \\ 1 & -\alpha_4 & 0 \\ 0 & 1 & -1 \end{pmatrix}.$$

The corresponding characteristic equation is

$$\begin{aligned}&|\lambda I - J_{E_1^{n_1,n_2}}| \\ &= \begin{vmatrix} \lambda-(\sigma_1-1)\alpha_2 & 0 & 0 \\ -1 & \lambda+\alpha_4 & 0 \\ 0 & -1 & \lambda+1 \end{vmatrix} \\ &= [\lambda-(\sigma_1-1)\alpha_2](\lambda+\alpha_4)(\lambda+1) \\ &= 0.\end{aligned}$$

When $\sigma_1 < 1$, the roots of the above equation have negative real parts. Thus, the system (2) is locally asymptotically stable at $E_1^{n_1,n_2}$ if $\sigma_1 < 1$.

(2) Before we discuss Theorem 3(2), we first prove that when $\sigma_2 > \frac{n_2 K}{(n_2-1)^{\frac{n_2-1}{n_2}}}$, there exist two positive real roots, denoted by $\overline{y}_{21}^{n_1,n_2}$ and $\overline{y}_{22}^{n_1,n_2}$, for the equation

$$\overline{y}^{n_2} - \sigma_2 \overline{y}^{n_2-1} + K^{n_2} = 0. \tag{C.1}$$

For discussion purposes, we let $0 < \overline{y}_{21}^{n_1,n_2} < \overline{y}_{22}^{n_1,n_2}$.

When $\overline{x} = 0$ and $\overline{z} = \overline{y} \neq 0$, we have $\frac{\sigma_2 \overline{y}^{n_2}}{K^{n_2}+\overline{y}^{n_2}} - \overline{y} = 0$ from $\frac{d\overline{y}}{dt} = 0$, then $\overline{y}^{n_2} - \sigma_2 \overline{y}^{n_2-1} + K^{n_2} = 0$. Set

$$f(\overline{y}) = \overline{y}^{n_2} - \sigma_2 \overline{y}^{n_2-1} + K^{n_2},$$

then

$$f'(\overline{y}) = n_2 \overline{y}^{n_2-1} - (n_2-1)\sigma_2 \overline{y}^{n_2-2}.$$

Let $f'(\overline{y}) = 0$, then $\overline{y} = \frac{n_2-1}{n_2}\sigma_2$. When $0 < \overline{y} < \frac{n_2-1}{n_2}\sigma_2$, $f'(\overline{y}) < 0$, and when $\overline{y} > \frac{n_2-1}{n_2}\sigma_2$, $f'(\overline{y}) > 0$.

Considering $f(0) > 0$ and $f(+\infty) > 0$, when $f(\frac{n_2-1}{n_2}\sigma_2) < 0$, i.e. $\sigma_2 > \frac{n_2 K}{(n_2-1)^{\frac{n_2-1}{n_2}}}$, Eq. (C.1) will have two different positive real roots, denoted by $\overline{y}_{21}^{n_1,n_2}$ and $\overline{y}_{22}^{n_1,n_2}$ respectively.

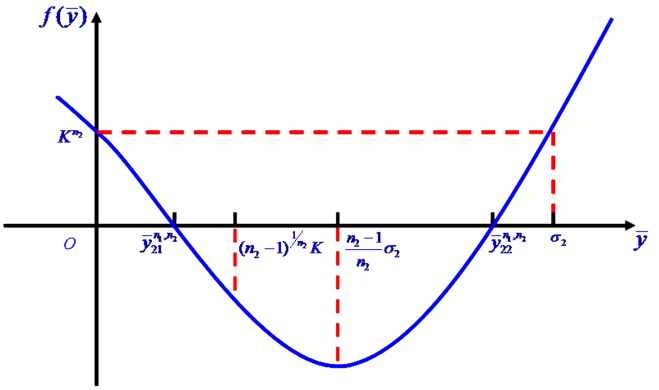

Fig. 14. When $\sigma_2 > \frac{n_2 K}{(n_2-1)^{\frac{n_2-1}{n_2}}}$, then $0 < \overline{y}_{21}^{n_1,n_2} < (n_2-1)^{\frac{1}{n_2}}K < \frac{n_2-1}{n_2}\sigma_2 < \overline{y}_{22}^{n_1,n_2} < \sigma_2$.

Let $\overline{y}_{21}^{n_1,n_2} < \overline{y}_{22}^{n_1,n_2}$. Thus, when $\sigma_2 > \frac{n_2 K}{(n_2-1)^{\frac{n_2-1}{n_2}}}$, then (Fig. 14)

$$0 < \overline{y}_{21}^{n_1,n_2} < \frac{n_2-1}{n_2}\sigma_2 < \overline{y}_{22}^{n_1,n_2} < \sigma_2.$$

Now, we prove that the EP $E_{21}^{n_1,n_2}$ is always unstable.

The Jacobi matrix at $E_{21}^{n_1,n_2}$ ($\overline{x}_{21}^{n_1,n_2} = 0$, $\overline{y}_{21}^{n_1,n_2} = \overline{z}_{21}^{n_1,n_2}$) is

$$J_{E_{21}^{n_1,n_2}} = \begin{pmatrix} \frac{\sigma_1\alpha_2}{1+(\overline{z}_{21}^{n_1,n_2})^{n_1}} - \alpha_2 & 0 & 0 \\ 1 & \frac{n_2\sigma_2\alpha_4 K^{n_2}(\overline{y}_{21}^{n_1,n_2})^{n_2-1}}{[K^{n_2}+(\overline{y}_{21}^{n_1,n_2})^{n_2}]^2} - \alpha_4 & 0 \\ 0 & 1 & -1 \end{pmatrix}.$$

The corresponding characteristic equation is

$$|\lambda I - J_{E_{21}^{n_1,n_2}}| = \begin{vmatrix} \lambda + \alpha_2 - \frac{\sigma_1\alpha_2}{1+(\overline{z}_{21}^{n_1,n_2})^{n_1}} & 0 & 0 \\ -1 & \lambda + \alpha_4 - \frac{n_2\sigma_2\alpha_4 K^{n_2}(\overline{y}_{21}^{n_1,n_2})^{n_2-1}}{[K^{n_2}+(\overline{y}_{21}^{n_1,n_2})^{n_2}]^2} & 0 \\ 0 & -1 & \lambda+1 \end{vmatrix}$$

$$= \left[\lambda + \alpha_2 - \frac{\sigma_1\alpha_2}{1+(\overline{z}_{21}^{n_1,n_2})^{n_1}}\right]\left\{\lambda + \alpha_4 - \frac{n_2\sigma_2\alpha_4 K^{n_2}(\overline{y}_{21}^{n_1,n_2})^{n_2-1}}{[K^{n_2}+(\overline{y}_{21}^{n_1,n_2})^{n_2}]^2}\right\}(\lambda+1)$$

$$= \left[\lambda + \alpha_2 - \frac{\sigma_1\alpha_2}{1+(\overline{y}_{21}^{n_1,n_2})^{n_1}}\right]\left\{\lambda + \alpha_4 - \frac{n_2\sigma_2\alpha_4 K^{n_2}(\overline{y}_{21}^{n_1,n_2})^{n_2-1}}{[K^{n_2}+(\overline{y}_{21}^{n_1,n_2})^{n_2}]^2}\right\}(\lambda+1) = 0.$$

In the following, we show that the above equation always has a positive real root, in other words, the system (2) cannot be locally asymptotically stable at $E_{21}^{n_1,n_2}$.

Assume

$$\alpha_4 - \frac{n_2\sigma_2\alpha_4 K^{n_2}(\overline{y}_{21}^{n_1,n_2})^{n_2-1}}{[K^{n_2} + (\overline{y}_{21}^{n_1,n_2})^{n_2}]^2} \geq 0,$$

then

$$[K^{n_2} + (\overline{y}_{21}^{n_1,n_2})^{n_2}]^2 \geq n_2\sigma_2 K^{n_2}(\overline{y}_{21}^{n_1,n_2})^{n_2-1}.$$

Due to $(\overline{y}_{21}^{n_1,n_2})^{n_2} - \sigma_2(\overline{y}_{21}^{n_1,n_2})^{n_2-1} + K^{n_2} = 0$, the above inequality can be rewritten as

$$K^{n_2} + (\overline{y}_{21}^{n_1,n_2})^{n_2} \geq n_2 K^{n_2}.$$

Then the inequality $\overline{y}_{21}^{n_1,n_2} \geq (n_2-1)^{\frac{1}{n_2}} K$ must be satisfied.

However, when $\sigma_2 > \frac{n_2 K}{(n_2-1)^{\frac{n_2-1}{n_2}}}$,

$$\begin{aligned} & f((n_2-1)^{\frac{1}{n_2}} K) \\ &= [(n_2-1)^{\frac{1}{n_2}} K]^{n_2} - \sigma_2[(n_2-1)^{\frac{1}{n_2}} K]^{n_2-1} \\ &\quad + K^{n_2} \\ &= K^{n_2-1}[n_2 K - \sigma_2(n_2-1)^{\frac{n_2-1}{n_2}}] \\ &< 0. \end{aligned}$$

This indicates that Eq. (C.1) has a positive real root from 0 to $(n_2-1)^{\frac{1}{n_2}} K$, i.e. $0 < \overline{y}_{21}^{n_1,n_2} < (n_2-1)^{\frac{1}{n_2}} K$, which conflicts with $\overline{y}_{21}^{n_1,n_2} \geq (n_2-1)^{\frac{1}{n_2}} K$, i.e. the assumption $\alpha_4 - \frac{n_2\sigma_2\alpha_4 K^{n_2}(\overline{y}_{21}^{n_1,n_2})^{n_2-1}}{[K^{n_2}+(\overline{y}_{21}^{n_1,n_2})^{n_2}]^2} \geq 0$ is wrong.

Therefore, the above characteristic equation for the non-negative EP $E_{21}^{n_1,n_2}$ always has a positive real root which means that the system (2) cannot be locally asymptotically stable at $E_{21}^{n_1,n_2}$, that is, $E_{21}^{n_1,n_2}$ is always unstable.

(3) The Jacobi matrix at $E_{22}^{n_1,n_2}$ is

$$J_{E_{22}^{n_1,n_2}} = \begin{pmatrix} \frac{\sigma_1\alpha_2}{1+(\overline{z}_{22}^{n_1,n_2})^{n_1}} - \alpha_2 & 0 & 0 \\ 1 & \frac{n_2\sigma_2\alpha_4 K^{n_2}(\overline{y}_{22}^{n_1,n_2})^{n_2-1}}{[K^{n_2}+(\overline{y}_{22}^{n_1,n_2})^{n_2}]^2} - \alpha_4 & 0 \\ 0 & 1 & -1 \end{pmatrix}.$$

The corresponding characteristic equation is

$$\begin{aligned} |\lambda I - J_{E_{22}^{n_1,n_2}}| &= \begin{vmatrix} \lambda + \alpha_2 - \frac{\sigma_1\alpha_2}{1+(\overline{z}_{22}^{n_1,n_2})^{n_1}} & 0 & 0 \\ -1 & \lambda + \alpha_4 - \frac{n_2\sigma_2\alpha_4 K^{n_2}(\overline{y}_{22}^{n_1,n_2})^{n_2-1}}{[K^{n_2}+(\overline{y}_{22}^{n_1,n_2})^{n_2}]^2} & 0 \\ 0 & -1 & \lambda+1 \end{vmatrix} \\ &= \left[\lambda + \alpha_2 - \frac{\sigma_1\alpha_2}{1+(\overline{z}_{22}^{n_1,n_2})^{n_1}}\right]\left\{\lambda + \alpha_4 - \frac{n_2\sigma_2\alpha_4 K^{n_2}(\overline{y}_{22}^{n_1,n_2})^{n_2-1}}{[K^{n_2}+(\overline{y}_{22}^{n_1,n_2})^{n_2}]^2}\right\}(\lambda+1) = 0 \\ &= \left[\lambda + \alpha_2 - \frac{\sigma_1\alpha_2}{1+(\overline{y}_{22}^{n_1,n_2})^{n_1}}\right]\left\{\lambda + \alpha_4 - \frac{n_2\sigma_2\alpha_4 K^{n_2}(\overline{y}_{22}^{n_1,n_2})^{n_2-1}}{[K^{n_2}+(\overline{y}_{22}^{n_1,n_2})^{n_2}]^2}\right\}(\lambda+1) = 0. \end{aligned}$$

We know that the system (2) is locally asymptotically stable at $E_{22}^{n_1,n_2}$ if the roots of the above equation have negative real parts, indicating that the two conditions,

$$\alpha_4 - \frac{n_2\sigma_2\alpha_4 K^{n_2}(\overline{y}_{22}^{n_1,n_2})^{n_2-1}}{[K^{n_2}+(\overline{y}_{22}^{n_1,n_2})^{n_2}]^2} > 0 \tag{C.2}$$

and

$$\sigma_1 < 1 + (\overline{y}_{22}^{n_1,n_2})^{n_1}, \tag{C.3}$$

must be satisfied.

First, we look for the conditions satisfying the inequality (C.2), i.e.

$$[K^{n_2} + (\overline{y}_{22}^{n_1,n_2})^{n_2}]^2 > n_2\sigma_2 K^{n_2}(\overline{y}_{22}^{n_1,n_2})^{n_2-1}.$$

Due to $(\overline{y}_{22}^{n_1,n_2})^{n_2} - \sigma_2(\overline{y}_{22}^{n_1,n_2})^{n_2-1} + K^{n_2} = 0$, the above inequality can be rewritten as

$$K^{n_2} + (\overline{y}_{22}^{n_1,n_2})^{n_2} > n_2 K^{n_2},$$

i.e.

$$\overline{y}_{22}^{n_1,n_2} > (n_2-1)^{\frac{1}{n_2}} K.$$

Because $\overline{y}_{22}^{n_1,n_2} > \frac{n_2-1}{n_2}\sigma_2$ and $\sigma_2 > \frac{n_2 K}{(n_2-1)^{\frac{n_2-1}{n_2}}}$ (Fig. 14), then

$$\overline{y}_{22}^{n_1,n_2} > \frac{n_2-1}{n_2}\frac{n_2 K}{(n_2-1)^{\frac{n_2-1}{n_2}}},$$

i.e.

$$\overline{y}_{22}^{n_1,n_2} > (n_2-1)^{\frac{1}{n_2}} K.$$

Thus, when $\sigma_2 > \frac{n_2 K}{(n_2-1)^{\frac{n_2-1}{n_2}}}$, the inequality (C.2) can be satisfied.

Second, to satisfy (C.3), i.e.

$$\overline{y}_{22}^{n_1,n_2} > (\sigma_1-1)^{\frac{1}{n_1}},$$

we must satisfy $f((\sigma_1-1)^{\frac{1}{n_1}}) < 0$ when $(\sigma_1-1)^{\frac{1}{n_1}} \geq \frac{n_2-1}{n_2}\sigma_2$ or $f'((\sigma_1-1)^{\frac{1}{n_1}}) < 0$ when $(\sigma_1-1)^{\frac{1}{n_1}} < \frac{n_2-1}{n_2}\sigma_2$ from Fig. 14.

When $(\sigma_1-1)^{\frac{1}{n_1}} \geq \frac{n_2-1}{n_2}\sigma_2$ and $f((\sigma_1-1)^{\frac{1}{n_1}}) < 0$, we have

$$\frac{K^{n_2} + (\sigma_1-1)^{\frac{n_2}{n_1}}}{(\sigma_1-1)^{\frac{n_2-1}{n_1}}} < \sigma_2 \leq \frac{n_2}{n_2-1}(\sigma_1-1)^{\frac{1}{n_1}}.$$

Or when $(\sigma_1-1)^{\frac{1}{n_1}} < \frac{n_2-1}{n_2}\sigma_2$ and $f'((\sigma_1-1)^{\frac{1}{n_1}}) < 0$, we have

$$\sigma_2 > \frac{n_2}{n_2-1}(\sigma_1-1)^{\frac{1}{n_1}}. \tag{C.4}$$

That is, when $\sigma_1 \geq 1 + (n_2-1)^{\frac{n_1}{n_2}} K^{n_1}$ and $\sigma_2 > \frac{K^{n_2} + (\sigma_1-1)^{\frac{n_2}{n_1}}}{(\sigma_1-1)^{\frac{n_2-1}{n_1}}}$, or when $\sigma_1 < 1 + (n_2-1)^{\frac{n_1}{n_2}} K^{n_1}$ and $\sigma_2 > \frac{n_2}{n_2-1}(\sigma_1-1)^{\frac{1}{n_1}}$, we have $\overline{y}_{22}^{n_1,n_2} > (\sigma_1-1)^{\frac{1}{n_1}}$, i.e. the inequality (C.3) can be established.

Taking into account $\sigma_2 > \frac{n_2 K}{(n_2-1)^{\frac{n_2-1}{n_2}}}$, the inequality (C.4) always holds when $\sigma_1 < 1 + (n_2-1)^{\frac{n_1}{n_2}} K^{n_1}$. Thus, when $\sigma_1 \geq 1 + (n_2-1)^{\frac{n_1}{n_2}} K^{n_1}$ and $\sigma_2 > \frac{K^{n_2} + (\sigma_1-1)^{\frac{n_2}{n_1}}}{(\sigma_1-1)^{\frac{n_2-1}{n_1}}}$, or when $\sigma_2 > \frac{n_2 K}{(n_2-1)^{\frac{n_2-1}{n_2}}}$, then we can ensure the inequality (C.3).

In summary, if $\sigma_2 > \frac{n_2 K}{(n_2-1)^{\frac{n_2-1}{n_2}}}$ and $\sigma_2 > \frac{K^{n_2} + (\sigma_1-1)^{\frac{n_2}{n_1}}}{(\sigma_1-1)^{\frac{n_2-1}{n_1}}}$ ($\sigma_1 \geq 1 + (n_2-1)^{\frac{n_1}{n_2}} K^{n_1}$), the system (2) is locally asymptotically stable at $E_{22}^{n_1,n_2}$.

(4) The Jacobi matrix at $E_3^{n_1,n_2}$ is

$$J_{E_3^{n_1,n_2}} = \begin{pmatrix} \frac{\sigma_1\alpha_2}{1+(\overline{z}_3^{n_1,n_2})^{n_1}} - \alpha_2 & 0 & -\frac{n_1\sigma_1\alpha_2\overline{x}_3^{n_1,n_2}(\overline{z}_3^{n_1,n_2})^{n_1-1}}{[1+(\overline{z}_3^{n_1,n_2})^{n_1}]^2} \\ 1 & \frac{n_2\sigma_2\alpha_4 K^{n_2}(\overline{y}_3^{n_1,n_2})^{n_2-1}}{[K^{n_2}+(\overline{y}_3^{n_1,n_2})^{n_2}]^2} - \alpha_4 & 0 \\ 0 & 1 & -1 \end{pmatrix}.$$

The corresponding characteristic equation is

$$|\lambda I - J_{E_3^{n_1,n_2}}| = \begin{vmatrix} \lambda + \alpha_2 - \frac{\sigma_1\alpha_2}{1+(\overline{z}_3^{n_1,n_2})^{n_1}} & 0 & \frac{n_1\sigma_1\alpha_2\overline{x}_3^{n_1,n_2}(\overline{z}_3^{n_1,n_2})^{n_1-1}}{[1+(\overline{z}_3^{n_1,n_2})^{n_1}]^2} \\ -1 & \lambda + \alpha_4 - \frac{n_2\sigma_2\alpha_4 K^{n_2}(\overline{y}_3^{n_1,n_2})^{n_2-1}}{[K^{n_2}+(\overline{y}_3^{n_1,n_2})^{n_2}]^2} & 0 \\ 0 & -1 & \lambda+1 \end{vmatrix}$$

$$= \left(\lambda + \alpha_2 - \frac{\sigma_1\alpha_2}{1 + (\overline{z}_3^{n_1,n_2})^{n_1}}\right)\left\{\lambda + \alpha_4 - \frac{n_2\sigma_2\alpha_4 K^{n_2}(\overline{y}_3^{n_1,n_2})^{n_2-1}}{[K^{n_2} + (\overline{y}_3^{n_1,n_2})^{n_2}]^2}\right\}(\lambda+1)$$

$$+ \frac{n_1\sigma_1\alpha_2\overline{x}_3^{n_1,n_2}(\overline{z}_3^{n_1,n_2})^{n_1-1}}{[1 + (\overline{z}_3^{n_1,n_2})^{n_1}]^2}$$

$$= \lambda(\lambda+1)\left\{\lambda + \alpha_4 - \frac{n_2\sigma_2\alpha_4 K^{n_2}(\sigma_1-1)^{\frac{n_2-1}{n_1}}}{\left[K^{n_2} + (\sigma_1-1)^{\frac{n_2}{n_1}}\right]^2}\right\}$$

$$+ \frac{n_1\alpha_2\alpha_4(\sigma_1-1)\left[K^{n_2} + (\sigma_1-1)^{\frac{n_2}{n_1}} - \sigma_2(\sigma_1-1)^{\frac{n_2-1}{n_1}}\right]}{\sigma_1\left[K^{n_2} + (\sigma_1-1)^{\frac{n_2}{n_1}}\right]} = 0,$$

i.e.

$$\lambda^3 + \left\{1 + \alpha_4 - \frac{n_2\sigma_2\alpha_4 K^{n_2}(\sigma_1-1)^{\frac{n_2-1}{n_1}}}{\left[K^{n_2} + (\sigma_1-1)^{\frac{n_2}{n_1}}\right]^2}\right\}\lambda^2 + \left\{\alpha_4 - \frac{n_2\sigma_2\alpha_4 K^{n_2}(\sigma_1-1)^{\frac{n_2-1}{n_1}}}{\left[K^{n_2} + (\sigma_1-1)^{\frac{n_2}{n_1}}\right]^2}\right\}\lambda$$

$$+ \frac{n_1\alpha_2\alpha_4(\sigma_1-1)\left[K^{n_2} + (\sigma_1-1)^{\frac{n_2}{n_1}} - \sigma_2(\sigma_1-1)^{\frac{n_2-1}{n_1}}\right]}{\sigma_1\left[K^{n_2} + (\sigma_1-1)^{\frac{n_2}{n_1}}\right]} = 0.$$

To simplify the discussion, we let

$$\lambda^3 + P\lambda^2 + Q\lambda + R = 0,$$

where

$$P = 1 + \alpha_4 - \frac{n_2\sigma_2\alpha_4 K^{n_2}(\sigma_1-1)^{\frac{n_2-1}{n_1}}}{\left[K^{n_2} + (\sigma_1-1)^{\frac{n_2}{n_1}}\right]^2}, \quad Q = \alpha_4 - \frac{n_2\sigma_2\alpha_4 K^{n_2}(\sigma_1-1)^{\frac{n_2-1}{n_1}}}{\left[K^{n_2} + (\sigma_1-1)^{\frac{n_2}{n_1}}\right]^2}$$

and

$$R = \frac{n_1\alpha_2\alpha_4(\sigma_1-1)\left[K^{n_2} + (\sigma_1-1)^{\frac{n_2}{n_1}} - \sigma_2(\sigma_1-1)^{\frac{n_2-1}{n_1}}\right]}{\sigma_1\left[K^{n_2} + (\sigma_1-1)^{\frac{n_2}{n_1}}\right]}.$$

From the Routh–Hurwitz criterion [Dorf & Bishop, 2001], when $P > 0$, $Q > 0$, $R > 0$ and $PQ > R$, the roots of the characteristic equation have negative real parts, i.e. the system (2) is locally asymptotically stable at $E_3^{n_1,n_2}$. Obviously, if $Q > 0$, then $P > 0$. We assume $Q > 0$ and $PQ > R$, then

$$\left[K^{n_2} + (\sigma_1-1)^{\frac{n_2}{n_1}}\right]^2 > n_2\sigma_2 K^{n_2}(\sigma_1-1)^{\frac{n_2-1}{n_1}}$$

and

$$\left\{1 + \alpha_4 - \frac{n_2\sigma_2\alpha_4 K^{n_2}(\sigma_1-1)^{\frac{n_2-1}{n_1}}}{\left[K^{n_2} + (\sigma_1-1)^{\frac{n_2}{n_1}}\right]^2}\right\} \cdot \left\{\alpha_4 - \frac{n_2\sigma_2\alpha_4 K^{n_2}(\sigma_1-1)^{\frac{n_2-1}{n_1}}}{\left[K^{n_2} + (\sigma_1-1)^{\frac{n_2}{n_1}}\right]^2}\right\}$$

$$> \frac{n_1\alpha_2\alpha_4(\sigma_1-1)\left[K^{n_2} + (\sigma_1-1)^{\frac{n_2}{n_1}} - \sigma_2(\sigma_1-1)^{\frac{n_2-1}{n_1}}\right]}{\sigma_1\left[K^{n_2} + (\sigma_1-1)^{\frac{n_2}{n_1}}\right]},$$

i.e. $\sigma_2 < \frac{\left[K^{n_2}+(\sigma_1-1)^{\frac{n_2}{n_1}}\right]^2}{n_2K^{n_2}(\sigma_1-1)^{\frac{n_2-1}{n_1}}}$ and $\alpha_2 < C^{n_1,n_2}$, where

$$C^{n_1,n_2} = \frac{\left\{1+\alpha_4-\frac{n_2\sigma_2\alpha_4K^{n_2}(\sigma_1-1)^{\frac{n_2-1}{n_1}}}{\left[K^{n_2}+(\sigma_1-1)^{\frac{n_2}{n_1}}\right]^2}\right\}\cdot\left\{1-\frac{n_2\sigma_2K^{n_2}(\sigma_1-1)^{\frac{n_2-1}{n_1}}}{\left[K^{n_2}+(\sigma_1-1)^{\frac{n_2}{n_1}}\right]^2}\right\}}{\frac{n_1(\sigma_1-1)\left[K^{n_2}+(\sigma_1-1)^{\frac{n_2}{n_1}}-\sigma_2(\sigma_1-1)^{\frac{n_2-1}{n_1}}\right]}{\sigma_1\left[K^{n_2}+(\sigma_1-1)^{\frac{n_2}{n_1}}\right]}}.$$

In addition, due to the conditions of $\overline{x}_3^{n_1,n_2} > 0$, $\overline{y}_3^{n_1,n_2} > 0$ and $\overline{z}_3^{n_1,n_2} > 0$, then $\sigma_1 > 1$ and $\sigma_2 < \frac{K^{n_2}+(\sigma_1-1)^{\frac{n_2}{n_1}}}{(\sigma_1-1)^{\frac{n_2-1}{n_1}}}$.

Therefore, if

$$\sigma_1 > 1, \quad \sigma_2 < \min\left\{\frac{K^{n_2}+(\sigma_1-1)^{\frac{n_2}{n_1}}}{(\sigma_1-1)^{\frac{n_2-1}{n_1}}}, \frac{\left[K^{n_2}+(\sigma_1-1)^{\frac{n_2}{n_1}}\right]^2}{n_2K^{n_2}(\sigma_1-1)^{\frac{n_2-1}{n_1}}}\right\}$$

and $\alpha_2 < C^{n_1,n_2}$, the system (2) is locally asymptotically stable at $E_3^{n_1,n_2}$. ■